Journal: Nature Medicine

SUPPLEMENTARY INFORMATION

Title:

A molecularly engineered split reporter for imaging protein-protein interactions with positron emission tomography

Authors:
Tarik F. Massoud[1,2,3,4], Ramasamy Paulmurugan[3,4] & Sanjiv S. Gambhir[3,4,5]

Departments of [1]Radiology and [2]Oncology, University of Cambridge School of Clinical Medicine, Cambridge CB2 2QQ UK;
[3]Molecular Imaging Program at Stanford (MIPS), and Departments of [4]Radiology and [5]Bioengineering, Bio-X Program, Stanford University School of Medicine, Stanford, California 94305-5427 USA.

Correspondence should be addressed to S.S.G. (sgambhir@stanford.edu).

SUPPLEMENTARY INFORMATION

SUPPLEMENTARY METHODS

Details of the chemicals, enzymes, and reagents, as well as construction of all the plasmids and descriptions of cell culture and transfections can be found below, and elsewhere (**1**). To assess the PCA strategy using split TK fragments upon heterodimerization of FRB and FKBP12 in 293T cells, 40 nM final concentration of rapamycin were added immediately after transfection. The cells were assayed after 36 hr incubation at 37°C and in 5% CO_2.

Chemicals, enzymes and reagents

Restriction and modification enzymes, and T4 DNA ligase were purchased from New England Biolabs (Beverly, MA). PCR amplification was performed with TripleMaster Taq DNA polymerase purchased from Brinkmann Eppendorf (Hamburg, Germany). The CheckMate Mammalian two-hybrid kit containing vectors pBIND-*Id* and pACT-*MyoD* was purchased from Promega (Madison, WI). The plasmids pC_4EN-F1 (expressing FKBP12) and pC_4-R_HE (expressing FRB) were obtained from Ariad Pharmaceuticals, Inc. (Cambridge, MA), and pCMV-HSV1-*sr39tk* was a gift from Dr. Margaret Black (Washington State University, Pullman, WA). Superfect transfection reagent, plasmid extraction kits, and DNA gel extraction kits were purchased from Qiagen (Valencia, CA). Bacterial culture media were purchased from BD Diagnostic Systems (Sparks, MD). Lipofectamine 2000 transfection reagent, all animal cell culture media, fetal bovine serum, the antibiotics streptomycin and penicillin, and plastic wares for growing cell cultures were purchased from Invitrogen (Carlsbad, CA). Rapamycin was purchased from Sigma (St. Louis, MO), and [8-^{3}H]Penciclovir was obtained from Moravek Biochemicals (Brea, CA).

Construction of plasmids

Expression vectors to generate circularly permuted TK variants:

To construct five versions of TK with five different split sites **(Supplementary Fig. 1)**, five N-terminal fragments (*nTK*) and five C-terminal fragments (*cTK*) of the HSV1-*sr39tk (TK)* gene were amplified using the 5' end forward and 3' end reverse primers described in **Supplementary Table 1**, and pCMV-HSV1-*sr39tk* as template. For convenient cloning, the forward primer for the upstream gene (*cTK*) was introduced with an *Nhe*I restriction enzyme site and a start codon, both satisfying partial Kozak consensus sequence requirements for expression enhancement. The reverse primer of the upstream gene and the forward primer of the linker gene were introduced with a *BamH*I restriction enzyme site. The forward primer of the downstream gene (*nTK*) and the reverse primer of the linker gene were introduced with an *EcoRI* restriction enzyme site. The reverse primer of the downstream gene was introduced with a *XhoI* restriction enzyme site and a

stop codon. cDNA encoding the flexible linker $(GGGGS)_2$ was placed between the upstream and downstream genes in each cassette. The digested fragments were cloned into a pcDNA3.1(+) vector backbone at *Nhe*I/*Xho*I restriction enzyme sites. All cassettes were driven by a CMV promoter. Isolated plasmids were analyzed for the presence of inserts, and positive clones were confirmed for insert presence based on fragment size using restriction endonuclease analysis.

Expression vectors for the TK PCA strategy:

These vectors are shown schematically in **Fig. 1b**. To construct the vector *nTK-Id*, *nTK* and *Id* were amplified using the 5' end forward and 3' end reverse primers described in **Supplementary Table 2**, and pCMV-HSV1-*sr39tk* and pBIND-*Id* as templates, respectively. For convenient cloning, the forward primer for the upstream gene (*nTK*) was introduced with an *Nhe*I restriction enzyme site and a start codon, both satisfying partial Kozak consensus sequence requirements for expression enhancement. The reverse primer of the *nTK* and the forward primer of the *Id* gene, with an initial cDNA sequence encoding the flexible linker $(GGGGS)_2$, were introduced with an *EcoRI* restriction enzyme site. The reverse primer of *Id* gene was introduced with a *XhoI* restriction enzyme site and a stop codon. A similar strategy was used to construct *MyoD-cTK*, except that the reverse primer of *MyoD*, with a terminal cDNA sequence encoding the flexible linker $(GGGGS)_2$, and the forward primer of the *cTK* gene were introduced with a *BamH*I restriction enzyme site. The template used was pACT-*MyoD*. The digested fragments were cloned into a pcDNA3.1(+) vector backbone at *Nhe*I/*Xho*I restriction enzyme sites. Isolated plasmids were analyzed for the presence of inserts, and positive clones were confirmed for insert presence based on fragment size using restriction endonuclease analysis. Similar strategies were used to construct nTK-FRB and FKBP12-cTK. The human FRB fragment was amplified using the forward primer designed with *EcoRI* and the linker sequence $(GGGGS)_2$, and the reverse primer designed with *XhoI* and a stop codon by using the template vector provided by Ariad pharmaceuticals. The amplified fragment was cloned downstream of *nTK* fragment by using corresponding restriction enzymes. Similarly, the protein fragment FKBP12 was amplified using the forward primer designed with *NheI* and a start codon, and the reverse primer designed with *BamHI* by using the template provided by Ariad pharmaceuticals. The digested fragment was cloned upstream of *cTK* fragment by digesting with corresponding enzymes. Further details of the cloning methods and the primer sequences used are available upon request. Using similar cloning strategies, a further 6 variations on nTK-FRB and FKBP12-cTK were constructed to obtain protein chimeras with different orientations, as described below **(Supplementary Fig. 2)**. Expression vectors for the system that also employs an intermolecular PPI of hypoxia-inducible factor (its subunit 1α, HIF1α) and the von Hippel-Lindau tumor suppressor (VHL) are shown in **Fig. 3b**. The system that employs an intramolecular protein folding sensor is shown in **Fig. 3c**.

Expression vectors for TK fragment point mutations:

These vectors are shown schematically in **Supplementary Fig. 3.** To generate nTK with the point mutation V119C, site directed mutagenesis (kit obtained from Strategene, La Jolla, CA) was performed with the forward primer 5'gtaatgacaagcgcccagataaca and the reverse primer 5'gcacgccgcgtccccggccgatat synthesized at the Stanford Protein and Nucleic Acid Facility. Similarly, to generate cTK with the point mutation R318C, site directed mutagenesis was performed with the forward primer 5'cgtcttggccaaatgtctccgtcccatgc and the reverse primer 5'gcatgggacggagacatttggccaagacg. Isolated plasmids were analyzed for the presence of inserts, and positive clones were confirmed for insert presence based on fragment size using restriction endonuclease analysis. The mutants were verified by sequencing.

Expression vectors for preparing stable 293T cells:

To prepare stable 293T cells we constructed a single vector system expressing split TK fragments as well as the interacting proteins (**Supplementary Fig. 4)**. The above described pcDNA3.1 (puromycin) vector expressing $nTK_{(V119C)}$-FRB driven by a CMV promoter used for the transient expression study was digested with BglII restriction enzyme and dephosphorylated. The forward and reverse primers designed with BglII restriction enzyme sites on either side were used for the PCR amplification of a ubiquitin promoter (*p*Ubi) driving FKBP12-cTK (*p*Ubi-FKBP12-cTK). The BglII restriction enzyme digested PCR product was ligated into the BglII digested dephosphorylated pcDNA3.1(+)-$nTK_{(V119C)}$-FRB to construct pcDNA-*p*Ubi-FKBP12-cTK-*p*CMV-$nTK_{(V119C)}$-FRB. This vector was used for making stable 293T cells. A separate pcDNA3.1 (puromycin) vector containing the Firefly luciferase gene driven by a ubiquitin promoter (*p*Ubi) was used for making a different set of stable 293T cells expressing the Firefly luciferase enzyme.

Cell uptake studies

Uptake of [8-^{3}H]Penciclovir (0.76 μCi/ml, 1.5×10^{-5} mg/ml) was assessed 36 h after transient transfection of 293T cells. The cells were incubated at 37°C for 4 hours. At the end of this period, radioactivity in the medium was measured. The wells were washed with 1X PBS (pH 7.2), the cells were harvested and the cell-associated radioactivity was determined with a Beckman LS-9000 Liquid Scintillation Counter with Biosafe II (Research products International) scintillation fluid, as described previously[25]. Triplicate samples were evaluated for all uptake studies. The same wells were also used for determining total protein content[25]. Data are expressed as the net accumulation of probe in [dpm cells/dpm medium (at start of exposure)/μg protein] ± SE. For statistical analysis, the 2-tailed Student's *t* test was used. Differences were considered significant at $P < 0.05$.

Cell culture

Human embryonic kidney cancer 293T cells (ATCC, Manassas, VA) were grown in MEM medium supplemented with 10% FBS and 1% penicillin/streptomycin solution.

Cell transfection

Transfections were performed in 80% confluent 24 hrs old cultures of 293T cells. For transfection in 12-well culture plates, 250 ng/well of DNA were used when a single construct was used for transfection, giving a total of 500 ng/well when two constructs were combined in a co-transfection. For transfection with pCMV-HSV1-*sr39tk* alone (as a positive control), 500 ng/well were used. First, single transfections of circularly permuted variants of TK were performed. Next, to assess the PCA strategy using split TK fragments, co-transfection was performed with constructs 4 plus 5 **(Fig. 1b)**, and subsequently with constructs 2 plus 3 **(Fig. 1b)**, also using constructs 6 and 7 **(Fig. 1b)** as appropriate controls. For assessment of point mutatated variants of TK on functioning of the PCA strategy, we co-transfected constructs I and III, I and IV, II and III, II and IV **(Supplementary Fig. 3)**. Volumes of Superfect used were as recommended by the manufacturer. For heterodimerization of FRB and FKBP12 in cell culture, 40 nM final concentration of rapamycin were added immediately after transfection. The cells were assayed after 36 hr incubation at 37°C and in 5% CO_2.

Western immunoblotting

Stably transfected cell samples were also lysed and expression levels of FRB (mTOR) and FKBP12 (either endogenous or in their fusion with split TK fragments) in total lysates were determined by immunoblotting with anti-TK (1:500, Polyclonal, raised in rabbit) for nTK-FRB and FKBP12-cTK, anti-FRB (Cell Signaling) for cellular FRB (mTOR), anti-FKBP12 (Abcam) for cellular FKBP12, and anti-α-tubulin (Sigma) as an internal control for loading.

Rapamycin escalation dose study

Prior to microPET imaging in living mice these cells were also used in a cell-culture rapamycin escalation dose study where net accumulation of probe was measured against increasing rapamycin doses up to 100 nM. Furthermore, since ascomycin (FK506) competes with rapamycin for binding to FKBP12, we studied this competitive binding in these stably transfected 293T cells by adding escalating concentrations (from 0 to 16 μM) of ascomycin along with 40 nM rapamycin 36 h prior to *in vitro* [8-^{3}H]Penciclovir cell uptake assay.

Reversibility of the split TK PCA

We studied the reversibility of our PCA based on split TK using a ligand-reversible dimer of a mutant FKBP12 called F_M (F36M) that can be disrupted by FK506 (2). We fused F_M to split TK fragments and transiently expressed (0.5 μg DNA per well in a 12-well plate) the resulting chimeras, $nTK_{(V119C)}$-F_M and F_M-cTK, in a single vector in 293T cells. Twenty-four hours later we added FK506 to these cells and, using an *in vitro* [8-

^{3}H]Penciclovir cell uptake assay, measured either the time- or dose-dependent changes in homodimer dissociation and consequent diminished TK complementation.

MicroPET imaging in living mice

All animal handling and care was performed in accordance with Stanford University Animal Research Committee guidelines. For imaging studies using stable cell lines, five 12-week old female nude mice (*nu/nu*) were implanted subcutaneously over the left shoulder with 5×10^6 mock transfected 293T cells admixed with 50,000 293T stable cells expressing Firefly luciferase (see below), and subcutaneously over the right shoulder with 5×10^6 293T stable cells expressing both $nTK_{(V119C)}$-FRB and FKBP12-cTK admixed with 50,000 293T stable cells expressing Firefly luciferase. The cells were allowed to grow as tumors for 7 days (to ~0.3-0.4 cm in diameter). On day 8 mice were tail vein injected with 200 μCi of [^{18}F]-FHBG after undergoing anesthesia with 2% isoflurane in oxygen at 2 L/min. Three hours later, mice were microPET imaged in a spread prone position in a FOCUS microPET scanner (Concorde Microsystems, Knoxville, TN). Images were reconstructed using a three-dimensional filtered back projection and iterative maximum *a posteriori* algorithm, and no partial volume correction (**3**). Immediately after imaging the animals were intraperitoneally injected with 50 μg of rapamycin; 24 h later all the animals were re-subjected to microPET imaging as mentioned above. The animals were further injected with intraperitoneal 50 μg rapamycin for two more days at 24 h intervals and subjected to repeat microPET imaging. In a separate cohort of 4 control mice, the above temporal imaging studies were performed in an identical fashion except that no rapamycin was administered. The counts from regions of interest (ROI) were converted to the percentage injected dose per gram (%ID/g) of tumor using filtered back projection as described previously (**3**). This %ID/g is a measure of the amount of tracer accumulated in a given tissue site normalized to the injected amount and to the mass of the tissue examined. The FHBG accumulation (%ID/g) in the 293T tumor cells reflects their TK activity. For statistical analysis, the 2-tailed Student *t*-test was used. Differences were considered significant at $P < 0.05$.

For imaging in these 5 mice, 293T cells stably expressing Firefly luciferase enzyme were used as secondary gene marked cells to report on overall tumor viability when admixed with 293T cells stably expressing split TK plus the interacting proteins FRB and FKBP12 under study. We therefore used Firefly luciferase activity measured by optical CCD camera imaging as an indirect crude measure of the viability and adequacy of cell number of admixed 293T cells acting as the source of the microPET images. Details of optical imaging are as reported previously (**4**). We removed the tumors from the animals after microPET imaging for immunostaining to confirm the expression of split TK protein within the tumors.

Immunostaining of tumors for split TK expression

We removed the tumors from the animals after microPET imaging, embedded them in OCT in a plastic mold, and froze them in liquid nitrogen. The frozen blocks were sliced using a cryotome and slices were immunostained to confirm the expression of split TK

protein within the tumors. Tumor slices of 10 μm from both control (mock transfected 293T cells) and experimental (stable 293T cells with split TK) tumors were fixed on glass slides with acetone for 2 min, after which this was made to evaporate by keeping at room temperature for 10 min. The tissues were blocked by incubating with Tris-Buffered Saline with Tween (TBST) containing 2% bovine serum albumin (BSA) for 60 min at room temperature. The slides were further incubated in TBST with 2% BSA containing anti-TK antibody (1:500, Polyclonal, raised in rabbit) for an additional 60 min. The slides were washed three times (5 min each) with TBST. The slides were then incubated with TBST containing fluorescein-labeled goat anti-rabbit secondary antibody (1:200; Chemicon, Temicula, CA) for 60 min at room temperature. The washed slides were mounted with coverslips by using Cytoseal XYL (Microm International, Walldorf, Germany). Fluorescent microscopy (using an excitation filter 365 nm) of these cells was performed using an Axiovert 25 microscope (Carl Zeiss AG, Thornwood, NY) and micrographs were obtained at ×400 magnification using an AxioCam MRc camera (Bernried, Germany). See **Supplementary Fig. 5**.

SUPPLEMENTARY DISCUSSION

Typical protein-protein interactions (PPI) represent low level biological events, and are thus challenging to locate and image in intact living subjects. Therefore, we (**5**) and others (**6**) have recently directed considerable efforts toward exploiting the inherent high sensitivity (thought to be in the 10^{-15} to 10^{-17} mole/L range[11]) of optical bioluminescence imaging using cooled CCD cameras to image and quantify in living mice very low levels of visible light that mirror typical protein-protein interaction events. As such, we previously reported an inducible yeast two-hybrid system with Firefly luciferase (**7**), and a split Firefly luciferase PCA to study protein-protein interactions in cell lines, and to non-invasively image interactions in living mice (**4**). For similar reasons, we more recently developed a bioluminescence resonance energy transfer BRET2 system that uses Renilla luciferase (hRluc) protein and its substrate DeepBlueC as an energy donor, and a mutant green fluorescent protein (GFP^2) as the acceptor (**8**). Moreover, we devised an inducible split hRluc PCA bioluminescence assay to quantitatively measure real time protein-protein interactions in mammalian cells and to image these in living mice in the presence of the substrate coelenterazine (**9**). We, and others, previously reviewed these various techniques available for molecular imaging of protein-protein interactions in living subjects (**10-14**).

The overall advantages of noninvasive diagnostic molecular imaging technologies (such as the ability to assess whole body phenomena, repeatability, functionality, and quantification) could be made more apparent with even greater exploitation of the benefits and accuracy of each imaging modality. Unfortunately, significant limitations of optical bioluminescence imaging arise on account of the considerable attenuation of light in tissues deeper than 1 cm from the exterior (e.g., skin, mucosa, or an exteriorized surgical bed) and the lack of fully quantitative and truly tomographic capabilities (**15**). Moreover, the inability to compare signal from different locations owing to variable delivery of substrate, especially on occasion with coelenterazine, contributes further to its semi-quantitative nature. These relative concerns are also to be reckoned with the absence of an equivalent imaging modality readily applicable to human imaging studies, thus preventing potential future direct translation of developed experimental methods in mice for clinical use. There is therefore an urgent need to develop inherently more accurate, 'translatable', and quantitative noninvasive techniques that could be used to image protein-protein interactions deep within experimental small and large animals.

One such imaging modality is PET, which also has a relatively high sensitivity, in the range of 10^{-11} to 10^{-12} moles/L, mainly because it depends on coincidence detection of gamma rays for image generation, and attenuation factors can be precisely corrected in PET (**15**). The development of PET-based reporter gene expression imaging assays in the drug discovery and evaluation process is particularly advantageous because of the ability to validate them in cell culture, and, unlike optical imaging, to use them in a fully quantitative and truly tomographic manner in small animal models of disease (especially in transgenics). An added theoretical possibility might also include the future potential use of the same reporter probe in established clinical PET centers, assuming it would be possible to introduce reporter genes into humans as part of future gene and cellular therapies (**16-18**), or assuming intensive ongoing efforts to develop alternative simpler strategies for potential future human applications—such as the delivery of circulating

exogenous split reporter proteins into cells using leader peptide sequences—do bear fruit. Indeed, the ability to perform translational research from a cell culture setting to pre-clinical animal models to clinical applications is one of the most unique and powerful features of PET technology (**19**). In part owing to its sensitivity and its fully quantitative and tomographic nature, PET is probably the only noninvasive imaging technology that currently can be applied in humans for *in vivo* monitoring of reporter gene expression, and with the potential to image complex biological phenomena such as protein-protein interactions (**20**).

An intact TK reporter had been used previously in a modified mammalian two-hybrid system to non-invasively PET image PPIs confined to the nucleus (**21,22**). In this study we describe the molecular engineering rationale and construction of a novel *split* TK used in a PCA for *in vivo* PET molecular imaging of protein-protein interactions. This strategy is more advantageous, versatile, and with far greater potential applications than through use of a mammalian two-hybrid system in that it can image protein interactions throughout the cell and not just confined to interactions of nuclear proteins.

The principle of the protein-fragment complementation assay (PCA) strategy for detecting PPIs was first demonstrated by Pelletier et al. using the enzyme dihydrofolate reductase (DHFR) (**23**), following inspiration from a 1994 paper by Johnsson and Varshavsky describing what they called the 'ubiquitin split protein sensor' (**24**). The important general question in designing potentially interacting chimeras is how best to fuse the fragments of a split reporter to the interacting proteins, and specifically, what choices of N- or C-termini to use for this purpose. We studied all possible relative orientations of split TK and interacting protein fragments to determine the optimal orientation of chimeras for evaluation in this PCA assay. For the DHFR PCA strategy, Michnick et al. did not observe any difference in how the assays performed with diverse relative orientations of interacting proteins and attached split reporters, i.e. for DHFR the orientation of fusions was found to make little difference (**25,26**). It was suggested that for proteins with clear domains that are contiguous with their polypeptide sequence, such as DHFR, it might be likely that any configuration would work, since the domain topology can be formed from any configuration of fusions (**26**). In contrast, however, when a protein does not have a domain structure that is contiguous with its sequence e.g. β-lactamase, and for single domain proteins, e.g. GFP (**27**), then, one configuration/orientation might be favored over any other (**26**). This was found to be the case also in bacterial PCA strategies based on aminoglcoside phosphotransferase and hygromycin B phosphotransferase (**25**).

Circular permutation screen for candidate complementation domains of TK

To create a PCA based on TK, the first step was to identify sites where we could disrupt the primary amino acid sequence of TK to separate the enzyme into two complementary protein fragments. Ultimately, the best evidence for whether particular split reporter fragments will work is to determine whether the full polypeptide sequence can be circularly permuted at the proposed points of dissection: this has turned out to be the case for every enzyme that has been used to date in a PCA (**26**) Being formally equivalent to circularization of a polypeptide chain followed by a cleavage at a site different from the

original termini, a circular permutation places charged chain termini at new locations in a protein (**28**).

Since many circularly permuted proteins fold into stable, functional conformations, often both *in vitro* and *in vivo* (**28**), the development of a PCA can be assisted by using circular permutation to identify specific sites within a reporter protein that could be split to create two complementary protein fragments. When constructing circularly permuted variants, particular scrutiny is necessary in considering the distance between the natural N- and C-termini and the relative length of the peptide linker designed to span this distance, so as not to compromise the flexibility at the natural ends of the circular protein. It is surprisingly often observed in nature that the N- and C-termini of folded proteins reside in close proximity; indeed there is a significant preference for them to do so (**29**). Williams et al. have indicated that 9 residues seems to represent the minimum number required for a linker that does not introduce conformational strain in an average protein (**30**); this number can be derived by representing a random coil polypeptide by the worm-like chain model (**30**). Since the distance between the two termini of TK is unknown, we judged that the 15-residue linker used in circular permutation of TK should produce enough flexibility between its two natural termini.

The constituent subunits of TK display the general αβ folding pattern. Each αβ structure is made up of 15 α-helices and 7 β-sheets. A 5-stranded parallel β-sheet forms part of the core of the molecule, which contains 5 active sites (**31**) **(Supplementary Fig. 6)**. There are no long cleft-like peptide loop segments in its backbone amenable to single site cleavage, as was the case when splitting Firefly luciferase (**4**) or GAR transformylase (**25**). A full circular permutation analysis (e.g. previously undertaken in *E. Coli* disulphide oxidoreductase DsbA [189 residues long] (**32**), and in DHFR [159 residues long] (**33**)) involving every peptide bond in the TK molecule was deemed too exhaustive and impractical a proposition. Since there are no obvious structural clues from the TK molecule as to where to home in precisely in order to increase the likelihood of a successful cleavage, five potential cleavage sites were simultaneously investigated in a partial circular permutation analysis. None of the five sites chosen for splitting were within regions of periodic secondary structure; all were within disordered loop regions. Three split sites (between Ala152 and Pro153, Gly180 and Ser181, and Pro195 and Pro196) were within active sites of TK, and another two split sites (between Thr265 and Ala266, and Pro300 and Asn301) were outside its active sites. Two split sites (between Gly180 and Ser181, and Pro300 and Asn301) were in regions of the molecule at the dimerization interface with the opposing homodimer. All five split sites were present on the surface of TK **(Supplementary Fig. 7)**.

We produced all circular permuted genes using polymerase chain reaction to amplify the desired region of a tethered head to tail dimer gene derived from HSV1-*sr39tk* (*TK*), in the form N-[*cTK*]-C-linker-N-[*nTK*]-C, where *nTK* and *cTK* represent the portions of the HSV1-*sr39TK* gene proximal and distal to the split site, respectively. The tethered dimer gene contained a DNA sequence encoding a flexible 15-amino acid [$(GGGGS)_3$] linker that connects the natural N-terminus of one copy of *nTK* to the natural C-terminus of the second copy of *cTK*. The linker used is of standard composition, made of 3 repeats of a penta-peptide composed of glycine (a neutral/normophobic amino acid with the smallest molecular weight [75 Da] and smallest

side chains amongst all amino acids, and serine, also a neutral amino acid with the third smallest molecular weight of 105 Da). This linker has also been used by other workers, e.g. Michnick et al. (**25**), and Galarneau et al. (**34**). We studied the functional effects of the engineered five circularly permuted variants of TK using *in vitro* TK enzyme uptake assays in 293T cells, and by comparing the properties of these mutated proteins with the original TK. The circularly permuted variant $_{CP}TK_{265}$ (where the split site was between Thr265 and Ala266) was the only mutation to retain TK enzymatic activity (85.2%, as compared to full length normal HSV1-sr39TK). All other circularly permuted variants ($_{CP}TK_{152}$, $_{CP}TK_{180}$, $_{CP}TK_{195}$, $_{CP}TK_{300}$) were enzymatically inactive **(Supplementary Fig. 8)**.

Orientation of split TK fragments

The active site of TK consists of the substrate nucleoside-binding pocket and the ATP nucleotide binding loop, as well as providing the residues that are responsible for co-ordinating the magnesium counterion (**31**). Thus, TK is a multi-domain protein with clear domains that are contiguous with its polypeptide sequence, but starting at residue Arg46. Its domains are defined as CORE (the central 5 β-sheets: residues 46-81, 143-218, 227-250, 323-376), the NMP_{bind} domain (nucleoside monophosphate binding domain: residues 82-142), and the LID domain (peptide segment at the ATP-binding site: residues 219-226) (**31**). Therefore, although TK does possess clear domains that are contiguous with its polypeptide sequence, these domains are not present along the entire length of TK, but instead, are skewed away from the N-terminal of TK (**31**). Moreover, the two monomers align themselves in C_2 symmetry, a type of two-fold symmetry in which the units are related to one another by a two-fold axis (called a dyad axis), i.e. the two subunits are rotated 180 degrees from each other. Based on these two observations, we judged it likely that one configuration/orientation of interacting proteins relative to split reporters might be favored over any other for a PCA strategy based on split TK. Indeed, co-expression of nTK-FRB together with FKBP12-cTK gave the optimal orientation of chimeras in this PCA assay.

We next questioned if the construction of the chimeric proteins nTK-FRB and FKBP12-cTK, used to this point in testing complementation of split TK fragments, did indeed represent the optimal orientation of heterodimeric interacting proteins relative to attached split TK fragments. To evaluate the interaction of any two given chimeric proteins, we constructed all eight possible chimeras with upstream and downstream orientations of nTK or cTK relative to FRB or FKBP12 **(Supplementary Fig. 2)**. This allowed a study of all eight conceivable combinations of interacting protein chimeras upon co-transfection of constructs A and B, C and D, E and F, G and H, A and D, B and C, E and H, and F and G, as shown in **(Supplementary Fig. 2)**. The optimal combination was found to be nTK-FRB interacting with FKBP12-cTK (combination F+G) **(Supplementary Fig. 9)**, precisely the orientation chosen at the outset of the study. We deemed this the best of the eight combinations because it yielded the lowest level of complemented TK in the absence of rapamycin (14.8% of the enzyme activity of full length TK, but also 2.3-fold above mock transfection levels), and the largest relative gain (an ~3-fold induction, $P < 0.05$) in complemented TK activity after rapamycin administration (amounting to 46.1% of the enzyme activity of full length TK). Low restored enzyme activity levels in the absence of rapamycin and large gains after

rapamycin would constitute desirable features for optimal functioning of this PCA strategy. When tested in 293T cells other combinations resulted in higher absolute levels of complemented TK activity, but considerably elevated levels (above mock levels) were also present prior to addition of rapamycin.

Temporal changes in complementation of split TK fragments

We undertook to combine an analysis of the co-expression of the fusion proteins described above with a temporal study to show how the resulting TK complementation might develop over the first 60 hours following transient transfection in 293T cells. This tactic seemed necessary on account of the findings of Gautier et al. who demonstrated, using homo-FRET anisotropy decay of GFP-tagged TK molecules, that TK homodimerization can only be observed beyond 24 hours of transient transfection in Vero cells (**35**). Accordingly, TK would seem to exist as a monomer in the first 24 hours after transient transfection, and in a monomer/dimer equilibrium thereafter. Using the determined combination of optimally oriented chimeras we further studied the temporal changes in split TK complementation over the first 60 hours after transient transfection **(Supplementary Fig. 10).** We found the greatest amount of activity of intact TK was at 36 hours after transient transfection, presumably early during the onset of TK homodimerization. Three other observations were apparent at this time period: the overall degree of restored TK activity was small, there was only a small rise in TK complementation upon adding rapamycin, and TK complementation was also detectable prior to adding rapamycin.

Rapamycin dose for heterodimerization-induced complementation of split TK fragments

Although low levels of restored enzyme activity were obtained in previous successful PCAs (e.g., 20% restored activity was achieved for humanized Renilla luciferase when used with the FRB/FKBP12 system (**9**)) we investigated if this low level of TK complementation was possibly due to an inadequate dose of rapamycin incapable of fully mediating heterodimerization of FRB and FKBP12.

We had previously evaluated the optimal concentration of rapamycin for efficient heterodimerization-associated recovery of complemented synthetic Renilla luciferase activity when using the FRB/FKBP12 system in 293T cells (**36**). The optimal rapamycin dose for routine use was 20-40 nM per well in a 12-well plate. The dose of rapamycin used in the above-described temporal study of heterodimerization-associated recovery of complemented TK activity was this optimal dose of 40 nM per well in a 12-well plate. In a prior study, Remy and Michnick used 20 nM per well when evaluating a DHFR-based PCA system in CHO DUKX-B11 cells (**37**). We therefore compared in a separate study the complemented TK activity upon using 4 nM and 40 nM rapamycin per well in a 12-well plate **(Supplementary Fig. 11)**. The recovered TK activity with the larger rapamycin dose was only slightly higher. Therefore, the overall relatively low level of complemented TK activity observed with heterodimerization of FRB and FKBP12, using split TK at position 265/266, was not likely due to an inadequate dose of the dimerizer rapamycin. Despite rapamycin being a known cell-cycle inhibitor, 40 nM of rapamycin per well is known to be non-toxic to cells, since the typical EC_{50} necessary to arrest cell

division is about 50 times more than the concentration range used here (**38**). Indeed, the peak effects of induced heterodimerization of two proteins using rapamycin are generally seen at recommended concentrations of 50-100 nM (**39**).

Self-complementation of split TK fragments

In a PCA strategy, spontaneous unassisted folding of split reporter fragments would lead to a false-positive reporter signal, a situation that would hopelessly confound attempts at interpreting the presence or absence of a protein-protein interaction under study (**26**). In the previous experiment, self-complementation of TK fragments was evident from the presence of restored TK activity upon co-expressing nTK-FRB and FKBP12-cTK in the absence of rapamycin (32.2% of the levels of complementation achieved upon protein-protein interaction, for constructs F+G.

To confirm or refute this finding we performed a separate PCA study using another pair of known interacting proteins, after replacing FRB and FKBP12 with Id and MyoD respectively. MyoD and Id are members of the basic-helix-loop-helix family of nuclear transcription factors, and are known to strongly interact *in vivo* (**40**). We tested the interaction of Id and MyoD upon transient co-expression of the fusion proteins nTK-Id and MyoD-cTK in 293T cells, followed by an *in vitro* TK enzyme cellular uptake assay to detect dimerization-assisted complementation of the TK fragments **(Supplementary Fig. 12)**. Again, this same orientation of chimeras using Id and MyoD was used previously in PCAs with split Firefly luciferase (**4**) and Renilla luciferase (**9**). We compared this with complementation obtained using the previous chimeras containing FRB and FKBP12, before and after addition of rapamycin. As negative controls we also assayed for TK activity upon single- and co-expression of nTK and cTK fragments without any attached proteins to check whether any measured TK activity might originate in either the N-terminal or C-terminal fragments of TK alone, or perhaps by their spontaneous self-complementation even without attached proteins. The results confirmed the findings described above using the FRB/FKBP12/rapamycin system. However, no perceptible complementation of TK was seen upon interaction of Id and MyoD. We also recorded no activity from the nTK or the cTK fragments alone, but a significant amount of complemented TK was measured upon co-expression of nTK and cTK, providing further evidence for the likely presence of self-complementation of nTK and cTK obtained through cleavage of TK at position 265/266. This self-complementation was unassisted; it could be demonstrated in the absence as well as in the presence of interacting proteins.

Of note, since 293T cells are designed for multiepisomal replication and relatively high levels of protein expression, it is quite possible that this may have contributed to our observation of this spontaneous fragment complementation.

Although self complementing reporter fragments might be useful for assaying of other cellular and subcellular events, as recently published by us using split optical imaging reporters (**41**), self complementation is detrimental in the context of measuring protein-protein interactions. This is because when there is restored reporter activity upon an apparent protein-protein interaction it is not possible to ascertain if this is a consequence of the protein-protein interaction driving the complementation of split fragments, or if it follows self-complementation of these fragments, or both.

Interacting proteins sterically hinder complementation of split TK fragments

In a successful PCA strategy the efficiencies of complementation between the split reporter fragments must be equivalent once they have been brought together by interactions between alternative interaction partners, i.e. steric hindrance should be avoided (**42**). We reasoned that perhaps owing to the larger sizes of Id and MyoD (14 kDa and 35 kDa, respectively) relative to FRB and FKBP12 (10 kDa and 12 kDa, respectively) there might be an element of steric hindrance imposed by the interacting proteins on the split TK fragments in their attempt to complement. We tested the interaction of Id and its usual partner MyoD, as well as FRB and its usual partner FKBP12, upon transient co-expression of the respective fusion proteins in 293T cells, followed by an *in vitro* TK enzyme cellular uptake assay to detect dimerization-assisted complementation of the TK fragments. We compared this with complementation obtained following deliberate mismatching of interacting partners, such that the nTK-Id chimera was co-expressed with FKBP12-cTK, and nTK-FRB was co-expressed with MyoD-cTK **(Supplementary Fig. 13)**. The results indicated an interesting gradation in the level of complemented TK activity in relation to the size of the protein attached to nTK primarily (the larger the protein, the less enzyme activity obtained), and the size of the protein attached to cTK secondarily (also, the larger the protein, the less enzyme activity obtained). These findings indicate that some degree of steric hindrance by these particular interacting proteins might contribute to the overall lower levels than hoped for of complementation of the split TK fragments observed in this study.

We also showed the likelihood that interacting protein partners sterically hinder the complementation of split TK fragments to variable degrees, depending on the size of the interacting proteins. This might account in some measure for why there was a greater extent of TK fragment complementation when using FRB/FKBP12 than Id/MyoD as test proteins. Such a limitation in a PCA strategy may arise especially when interactions between large proteins or giant oligomeric proteins are being investigated. Under such circumstances, steric hindrance by the large proteins can possibly inhibit the interactions between the two separate reporter fragments.

TK fragment point mutations to optimize the split TK PCA strategy

We next investigated the possibility of diminishing self-complementation and augmenting PPI-induced complementation of split TK fragments by introducing two point mutations in the TK molecule. Degreve et al. had shown that the Arg-318 residue of TK is especially important for homodimerization (**43**). R318 hydrogen bonds with a water molecule, which in turn hydrogen bonds with the main chain carbonyl of the alanine residue at position 137 of the opposite monomer. Mutation of R318 leads to disruption of the interactions that stabilize the dimer and yields a predominant population of TK monomers. Arginine is a hydrophilic amino acid; we therefore point mutated this to a hydrophobic cysteine residue, yielding R318C. On the other hand, Wurth et al. have shown that the Val-119 residue of TK, one in each subunit of the dimer, and located in the NMP-binding domains, appear to be sufficiently close to each other to permit

disulfide bond formation when mutated into cysteines (**44**). This crosslinks the two monomers covalently, resulting in a mutant with properties identical to the original TK enzyme. We therefore point mutated V119 to a cysteine residue, yielding V119C. The nTK fragment containing the mutation V119C ($nTK_{(V119C)}$) was fused upstream of FRB, and cTK containing the mutation R318C ($cTK_{(R318C)}$) was fused downstream of FKBP12 **(Supplementary Fig. 3)**.

We next tested the interaction of FRB and FKBP12 upon transient co-expression of the appropriate pairs of fusion proteins from the available choices of nTK-FRB, FKBP12-cTK, $nTK_{(V119C)}$-FRB, and FKBP12-$cTK_{(R318C)}$ in 293T cells, followed by an *in vitro* TK enzyme cellular uptake assay to detect dimerization-assisted complementation of the TK fragments. The results indicated that no restored TK activity was detected whenever $cTK_{(R318C)}$ was one of the split reporter fragments **(Fig. 1c)**. This mutation prevented both self-complementation and PPI-assisted complementation, even in the presence of $nTK_{(V119C)}$, suggesting perhaps that the R318C mutation might have a dominant functional effect (TK monomerization) over the dimerizing effect of V119C. Alternatively, and as alluded to by Degreve et al. in a different context (**43**), R318C might result in an overall conformational change of the TK protein that, in the context of this study, might render it inactive. On the other hand, when $nTK_{(V119C)}$ was co-expressed with FKBP12-cTK (that is, in the absence of the R318C mutation), there was a prominent (41%) rise in the protein interaction-assisted level of TK complementation, consistently observed with repeated transient transfection experiments. This noticeable rise was at the limit of statistical significance ($P = 0.05$) when compared with the PCA without the V119C mutation. Self-complementation levels, however, still remained similar to those seen after co-expression of the standard nTK-FRB and FKBP12-cTK fusion proteins.

The exact reasons for this noted rise in complemented TK activity when using $nTK_{(V119C)}$ remain elusive. We know, for example, from the work of Wurth et al. that the cross-linked TK dimers have identical properties to TK in terms of expression yield, denaturing SDS PAGE gel electrophoresis, enzyme kinetics, CD spectra and thermal stability (**44**). We also know that TK does not have to dimerize to become active; the dimer is enzymatically even reported to be less efficient than the monomer (**44**). Regardless of the precise mechanisms involved, we considered the consistent perceptible rise in the degree of protein-protein interaction-assisted complementation of TK fragments when using $nTK_{(V119C)}$ to be useful, which potentially could be translated into a greater degree of imaging signal upon protein-protein interaction in a living subject than possibly seen with use of the non-mutated nTK fragment.

Characterization of 293T stable cells

We prepared 293T cells stably expressing $nTK_{(V119C)}$-FRB and FKBP12-cTK in a single vector **(Supplementary Fig. 4)** and tested them for the expression of split TK plus the interacting proteins using the *in vitro* [8-^{3}H]Penciclovir cell uptake assay before and after 36 h exposure of cells to rapamycin. Expression levels of FRB and FKBP12 (in their fusion form or endogenous to these stable cell) were determined in total cell lysates by immunoblotting with the corresponding antibodies, and were found to be adequate for use of these protein chimeras in a PCA strategy. Optical densitometry of the bands revealed

that FKBP12-cTK was expressed at a level only marginally above that of endogenous cellular FKBP12 (relative band intensities were 1.2:1.0). Various doses of rapamycin (a known cell-cycle inhibitor at high concentrations) up to the standard 40 nM dose used in this study had no effect on expression levels of these chimeras **(Supplementary Fig. 14 and 15).**

The cells selected and subsequently used for imaging also responded in a dose dependent manner to increasing rapamycin doses up to 100 nM when tested in a cell-culture rapamycin escalation dose study **(Supplementary Fig. 16)**. The rapamycin-induced TK activity of cells expressing the $nTK_{(V119C)}$-FRB and FKBP12-cTK fusions was consistent with the known pharmacological response, showing single-site quasi-saturable binding with a calculated dissociation constant, K_d of ~0.15 nM. We speculate that this value differs considerably from K_d values reported in the literature (**2**) because we used intact cells that required prolonged incubation with substrate to allow its transport across membranes and eventual intracellular phosphorylation, and not purified proteins in vitro, as performed by others (**45,46**). We further scrutinized the association of the rapamycin-FKBP12 complex with FRB because, should it be possible to demonstrate that the formation of this complex is directly induced by rapamycin and competitively inhibited by ascomycin (FK506), this would confirm that the observed complementation of split TK is driven by a specific molecular interaction (**2**). Since ascomycin competes with rapamycin for binding to FKBP12, we studied this competitive binding in these stably transfected 293T cells by adding escalating concentrations (from 0 to 16 μM) of ascomycin along with 40 nM rapamycin 36 h prior to *in vitro* [8-^{3}H]Penciclovir cell uptake assay. The results showed that increasing the concentration of ascomycin led to a reduction in TK complementation **(Supplementary Fig. 17)**, likely because it blocked the binding of rapamycin to FKBP12 and thus reduced the heterodimerization with FRB. Ascomycin prevented rapamycin-induced TK activity with an inhibition constant, K_i of ~9000 nM, somewhat different from values reported in the literature (**2,45**), likely for the same reasons outlined above. Given the particular increments we used in this study, the smallest concentration of ascomycin required to initiate the competitive inhibition of rapamycin was found to be 0.5 μM.

Reversibility of the split TK PCA

We separately studied the reversibility of our split TK-based PCA using a ligand-reversible dimer of a mutant FKBP12 called F_M (F36M) that can be disrupted by FK506 (**2**). We fused F_M to split TK fragments and transiently expressed the resulting chimeras, $nTK_{(V119C)}$-F_M and F_M-cTK, in a single vector in 293T cells. Twenty-four hours later we added FK506 to these cells and, using an *in vitro* [8-^{3}H]Penciclovir cell uptake assay, measured either the time- or dose-dependent changes in homodimer dissociation and consequent diminished TK complementation. Five μM FK506 resulted in dissociation of about two-thirds of complexes within 30 min, and incremental reduction of TK activity was observed with increasing doses of FK506 up to 5 μM (measured after 24 hr of exposure to this ligand) **(Supplementary Fig. 18 and 19).** This observed reversibility of

our PCA confirms that disassembly of the folded TK reporter is possible even after split TK fragments have complemented following a protein-protein interaction.

Unlike fluorescence microscopy-based techniques, detailed studies of the kinetics of protein-protein interactions, including analysis of split reporter complementation reversibility, have been limited to date. More specifically, although it is possible in all molecular imaging split reporter complementation systems developed so far to record the occurrence of a protein-protein interaction event (i.e., a hypothetical switch from 'off' [no interaction] to 'on' [interaction]), a relative limitation of these systems had been the inability to determine the consequences of an event where two protein interacting partners to which split reporters are fused cease to interact (i.e., a switch back to 'off' from the 'on' position). Such a recognized limitation of PCAs has been recently addressed by Remy and Michnick (**47**) who demonstrated reversibility of a PCA based on split *Gaussia* luciferase using the ligand-reversible F_M system, also used in this study. We too demonstrated the ability of our complemented split TK fragments to exhibit natural reversibility when driven by disassembly of attached interacting proteins. This will be very useful in future imaging studies of drug induction and inhibition, as well as kinetic studies of protein complex assembly and disassembly with the split TK PCA. These future experiments will also require assessment in several more cell lines, as well as with a greater variety of protein partners of different sizes and interaction affinities (weak transient to strong obligate), to establish further general applicability of this technique. These additional studies should also help to investigate the many other factors that could in theory have a bearing on data analysis and interpretation when imaging protein-protein interactions. These might include changes in the stability, solubility, enzymatic activity, and cellular localization of the complemented TK reporter. We are planning additional future studies that will assess potentially greater imaging sensitivity upon protein-protein interaction when using wild-type HSV1-TK (rather than HSV1-sr39TK) along with radiolabeled uracil nucleoside derivatives such as FIAU or FEAU, and when employing other molecular engineering strategies that can result in greater physical approximation of interacting protein partners, such as through use of protein chimeras containing long flexible linkers spanning the individual protein components under scrutiny. We previously developed such a system for improved optical imaging of protein-protein interactions (**48**).

MicroPET imaging in living mice

We used this mutated split TK in an *in vivo* PCA to quantitatively microPET image real time protein-protein interactions in 293T cells subcutaneously implanted in living mice. 293T cells were stably transfected with a single vector carrying $nTK_{(V119C)}$-FRB plus FKBP12-cTK and microPET imaging was performed after tail vein injection of the [^{18}F]-FHBG probe. The signal from each implant (demonstrated to contain equal viable cell counts using independent optical imaging) was quantified directly from the microPET images to determine the %ID/g for the FHBG probe. Mock transfected cells acted as a negative control. The mean %ID/g for FHBG accumulation in the cells transfected with $nTK_{(V119C)}$-FRB plus FKBP12-cTK increased over 5 days of daily rapamycin administration to a value of 4.37 ± 1.74, as compared to a background value of 0.28 ±

0.10 for the mock transfected cells. These results were statistically significant between experimental tumor and control groups ($P = 0.02$), demonstrating for the first time the feasibility of protein-protein interaction PET reporter complementation imaging in living subjects using the molecularly engineered split TK system described herein **(Fig. 4)**.

SUPPLEMENTARY FIGURES

Supplementary Fig. 1:

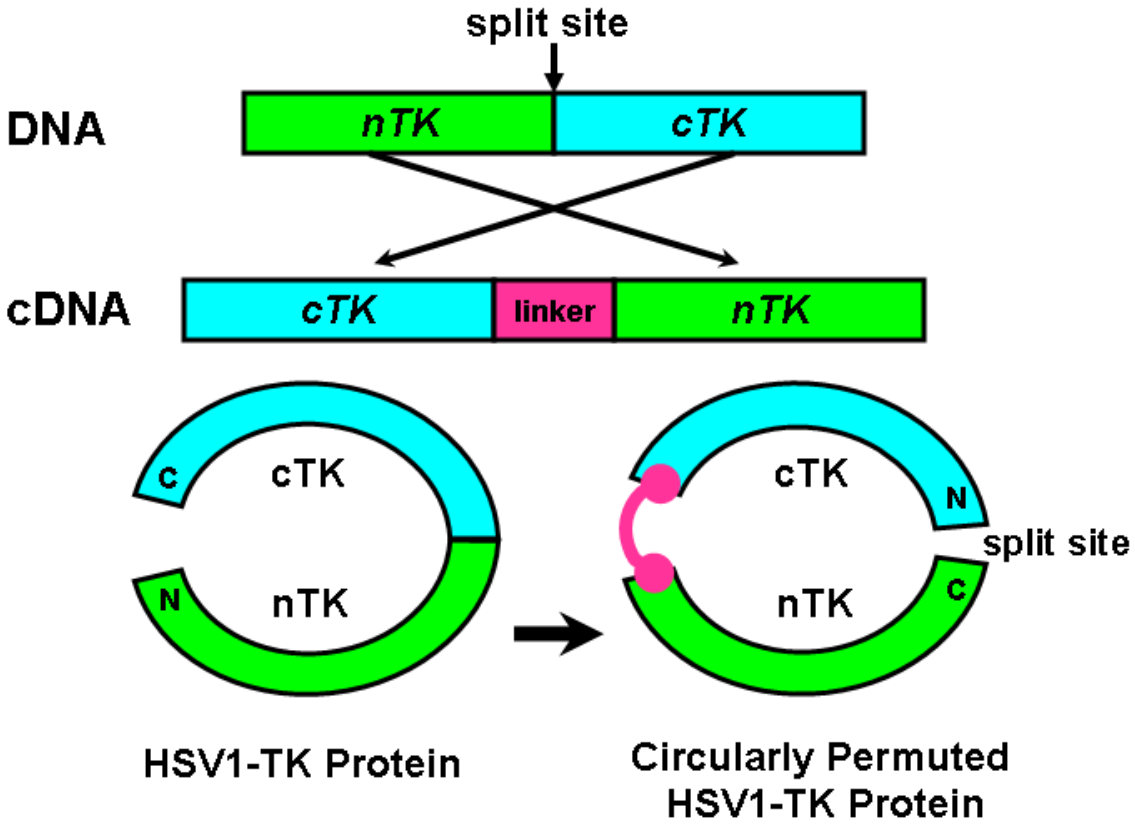

Circular permutation strategy for TK. Scheme of the construction of the five circularly permuted genes of HSV1-TK. cDNA fashioned from PCR products *cTK* and *nTK* are joined by a linker region. Each vector was cloned into a pcDNA3.1 (+) plasmid backbone, under control of a CMV promoter. The original protein termini are covalently linked to form a circular polypeptide. New termini are then created by cleavage of a peptide bond at a location along the backbone distant from the original termini.

Supplementary Fig. 2:

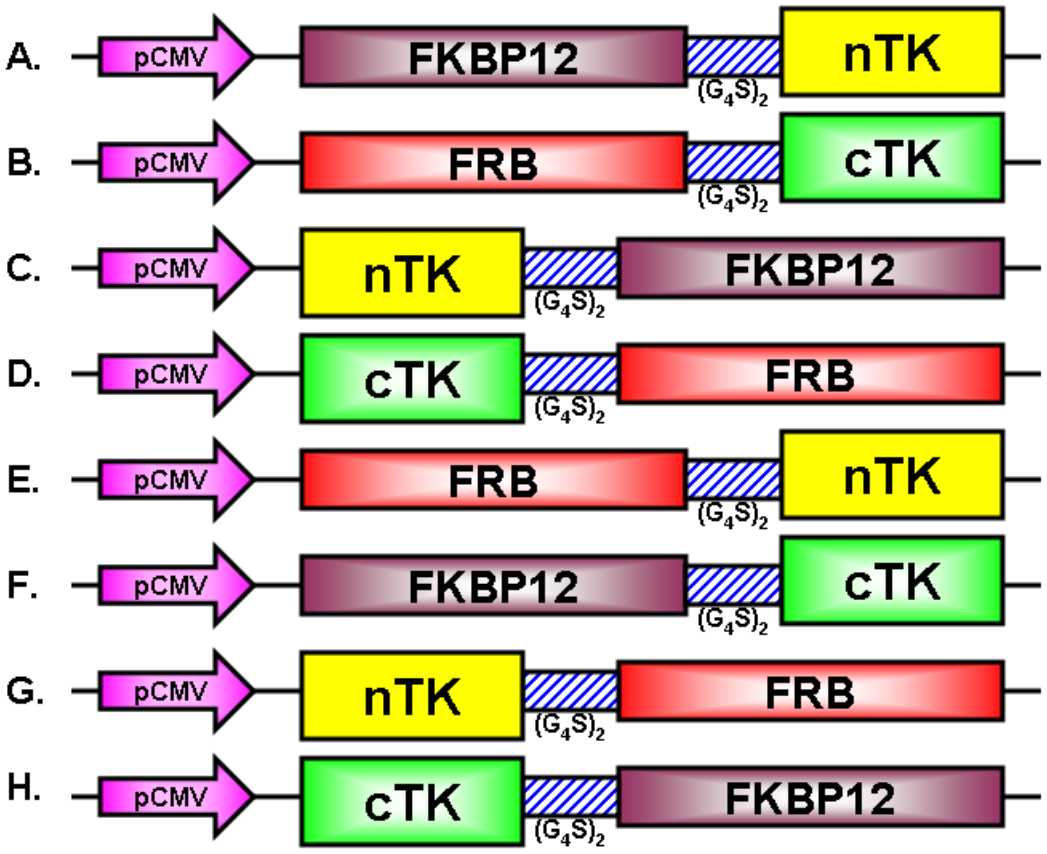

Schematic representation of the plasmid vector constructs made for transient expression of the eight genes transfected in combinations described in the text, for evaluation of the relative orientation of reporter fragments and interacting proteins on the functioning of the PCA strategy. Each construct was made by cloning into a pcDNA3.1 (+) plasmid backbone, under control of a CMV promoter.

Supplementary Fig. 3:

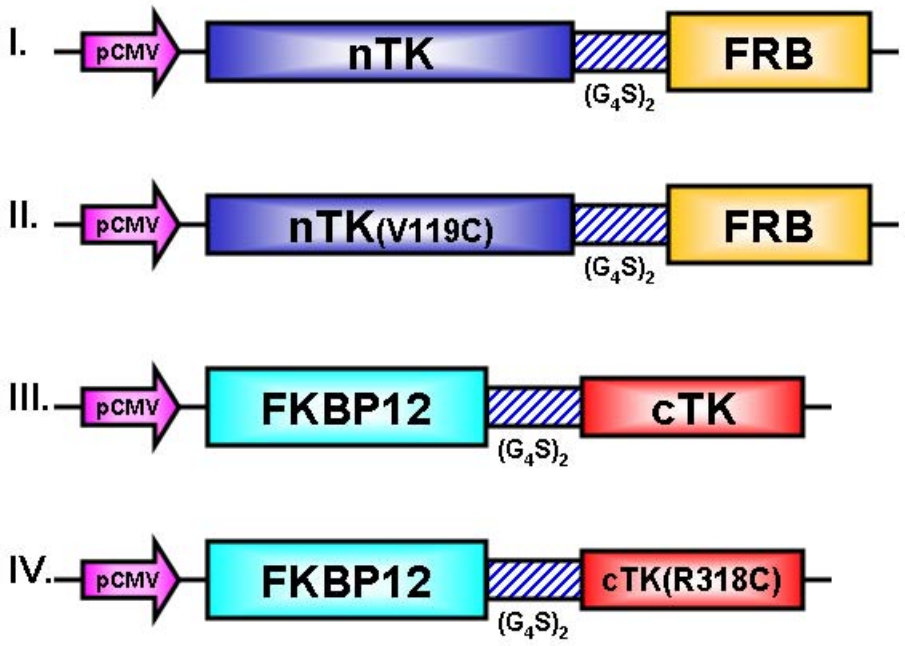

Schematic representation of the plasmid vector constructs made for transient expression of the four genes transfected in combinations described in the text, for evaluation of the PCA strategy after introducing point mutations V119C and R318C in the TK gene. Each vector was cloned into a pcDNA3.1 (+) plasmid backbone, under control of a CMV promoter.

Supplementary Fig. 4:

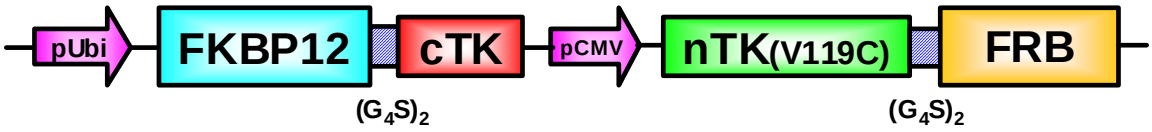

Schematic representation of the single plasmid vector construct made for stable expression of the four genes (two split TK and two interacting protein fragments) driven by pUbi and pCMV promoters, for evaluation of the PCA strategy after introducing the point mutation V119C in the nTK gene. This vector was cloned into a pcDNA3.1 (+) plasmid backbone.

Supplementary Fig. 5:

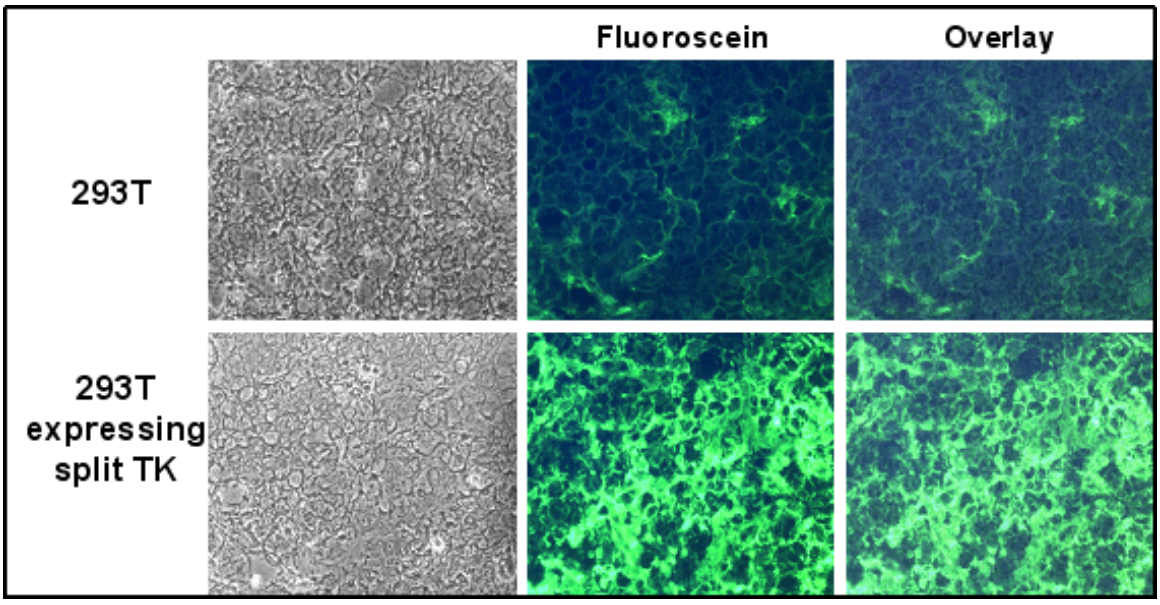

Fluorescence micrographs (×400 magnification) after immunohistochemical staining of control and experimental tumors shows considerable levels of TK protein expression from the tumors developed from 293T cells stably expressing split TK plus the interacting proteins, and not from the control mock transfected 293T cells.

Supplementary Fig. 6:

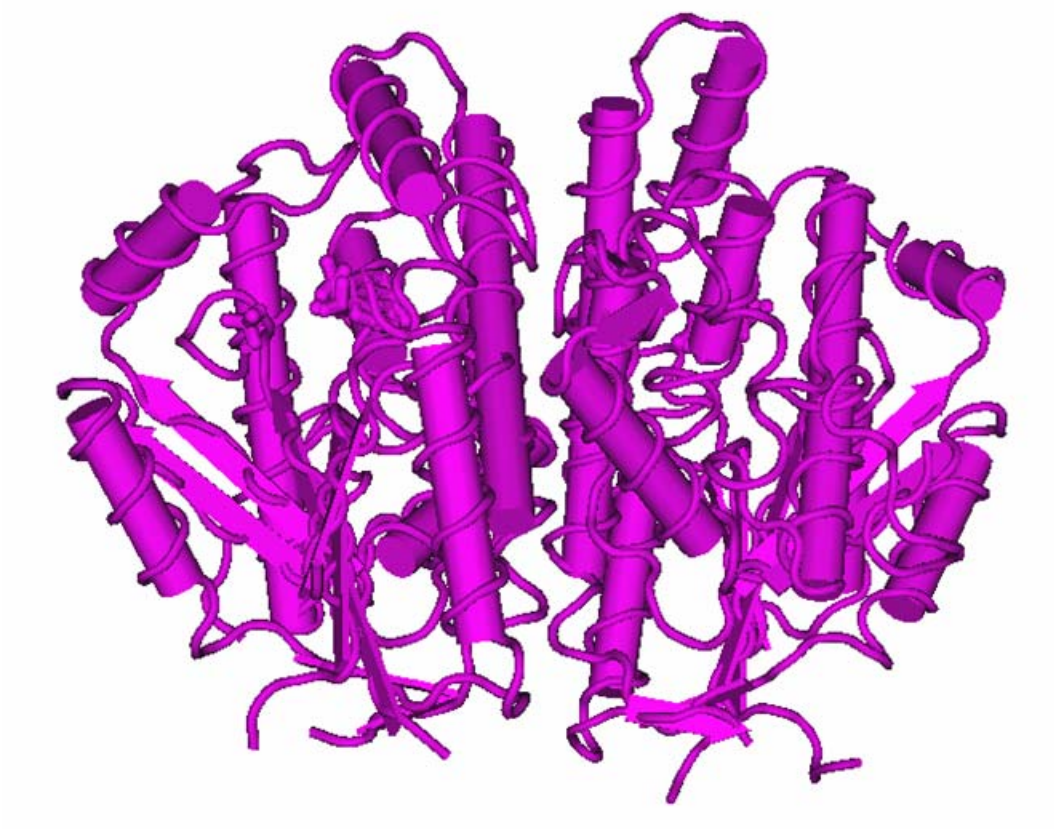

Ribbon diagram of the quaternary structure of the HSV1-TK homodimer. The constituent subunits of TK (376 amino acids long) display the general αβ folding pattern. Each αβ structure is made up of 15 α-helices and 7 β-sheets. A 5-stranded parallel β-sheet forms part of the core of the molecule, which contains 5 active sites.

Supplementary Fig. 7:

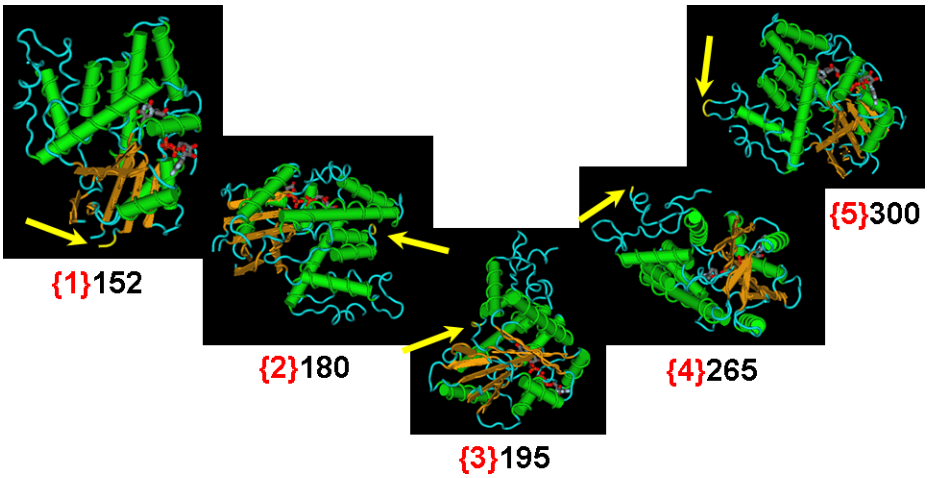

MASYPCHQHASAFDQAARSRGHSNRRTALRPRRQQEATEVRLEQKMPTLLRVYI
DGPHGMGKTTTTQLLVALGSRDDIVYVPEPMTYWRVLGASETIANIYTTQHRLDQG
EISAGDAAVVMTSAQITMGMPYAVTDAVLAPHIGGEAGSSHA{1}PPPALTLIFDRH
PIAALLCYPAARYLMG{2}SMTPQAVLAFVALIP{3}PTLPGTNIVLGALPEDRHIDRL
AKRQRPGERLDLAMLAAIRRVYGLLANTVRYLQCGGSWREDWGQLSGT{4}AVTP
QGAEPQSNAGPRPHIGETLFTLFRAPELLAP{5}NGDLYNVFAWALDVLAKRLRPM
HVFILDYDQSPAGCRDALLQLTSGMVQTHVTTPGSIPTICDLARTFAREMGEAH

Structure and circular permutation strategy for TK. Ribbon diagrams of five TK molecules rotated in space to show positions of the five chosen split sites (yellow arrows) in this study. These split sites are numbered in red and are also bracketed (in red) onto the primary sequence of TK. This is to demonstrate the relative positions of the split sites to β-pleated sheets (blue), α-helices (green), and the active sites of the enzyme (underlined). TK is 376 amino acids long.

Supplementary Fig. 8:

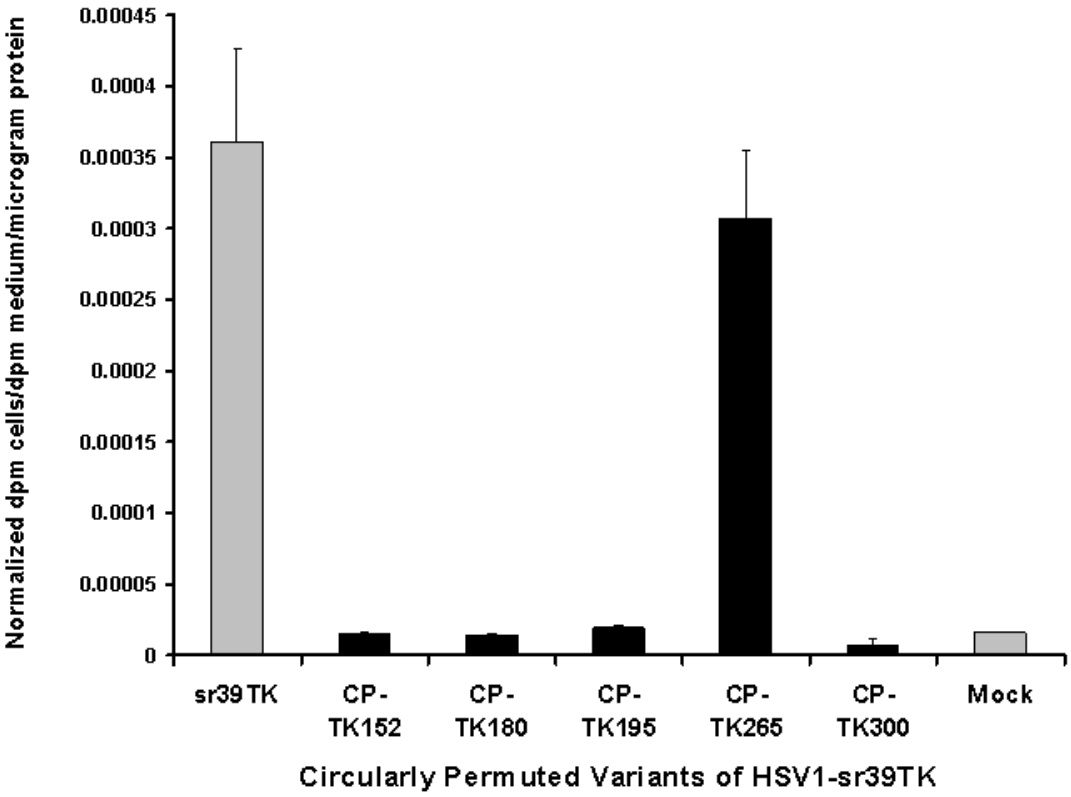

Graph to show enzyme activity of five circularly permuted variants of TK, measured by TK enzyme uptake (expressed as normalized dpm of cells/dpm in medium/microgram of protein) in transiently transfected 293T cells, with mock (negative) and full length HSV1-sr39TK (positive) controls. The error bar is the standard error of the mean for three samples.

Supplementary Fig. 9:

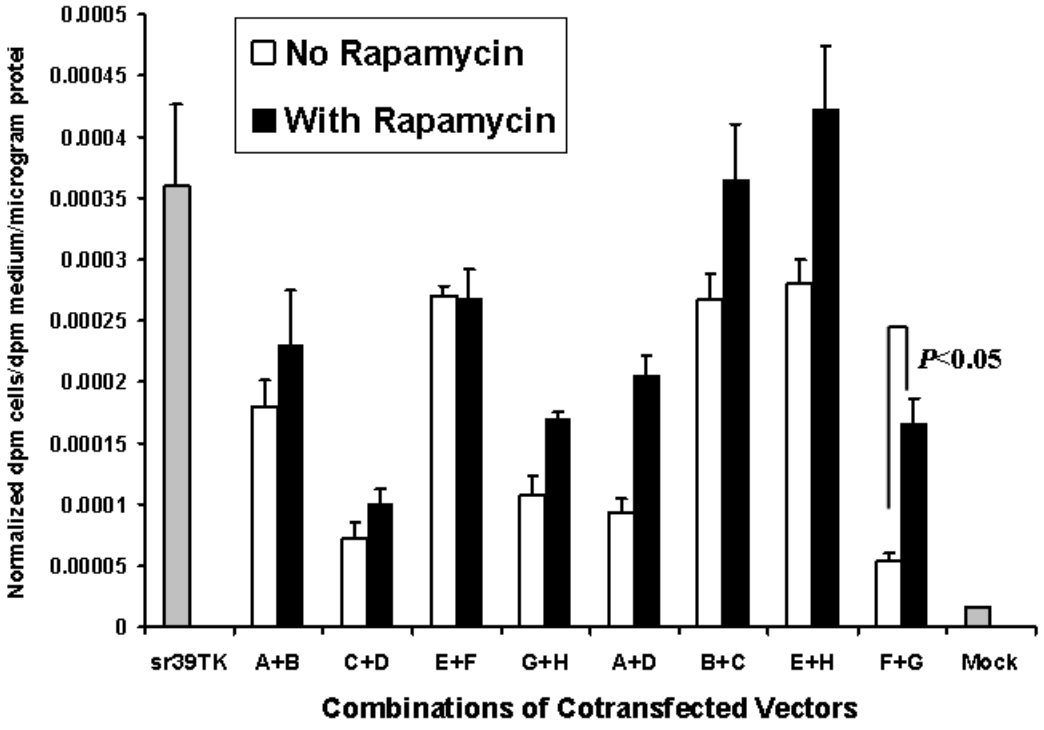

Graph to show comparison of coexpressed chimeras carrying nTK or cTK with FRB/FKBP12 (with and without rapamycin), to show the effect of relative orientation of reporter fragments and interacting proteins on enzyme activity of a PCA, measured by TK enzyme uptake (expressed as normalized dpm of cells/dpm in medium/microgram of protein) in transiently transfected 293T cells, with mock (negative) and full length HSV1-sr39TK (positive) controls. The error bar is the standard error of the mean for three samples. Letters denoting the various chimeras are as shown in Supplementary Fig. 2. There was a statistically significant increase in measured TK activity after co-transfecting chimeras F with G, upon addition of rapamycin.

Supplementary Fig. 10:

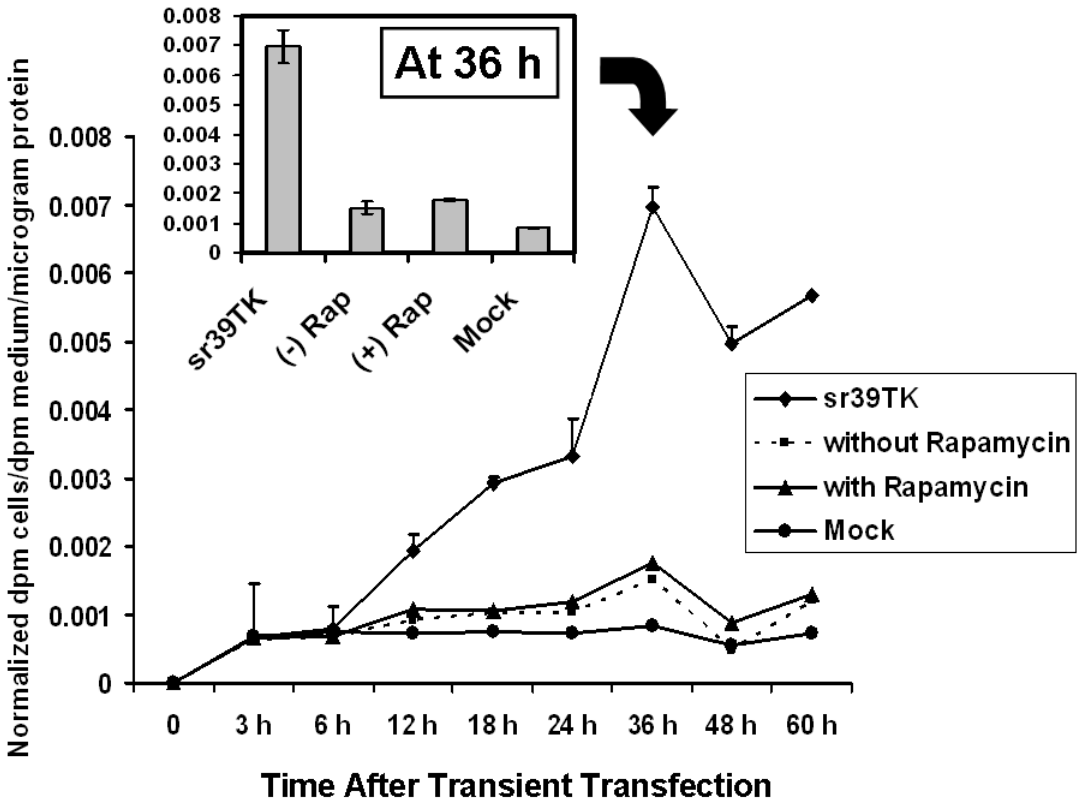

Graph to show time course of enzyme activity of a PCA using coexpressed chimeras carrying nTK or cTK with FRB/FKBP12 (with and without rapamycin), measured by TK enzyme uptake (expressed as normalized dpm of cells / dpm in medium /microgram of protein) in transiently transfected 293T cells, with mock (negative) and full length HSV1-sr39TK (positive) controls. The error bar is the standard error of the mean for three samples.

Supplementary Fig. 11:

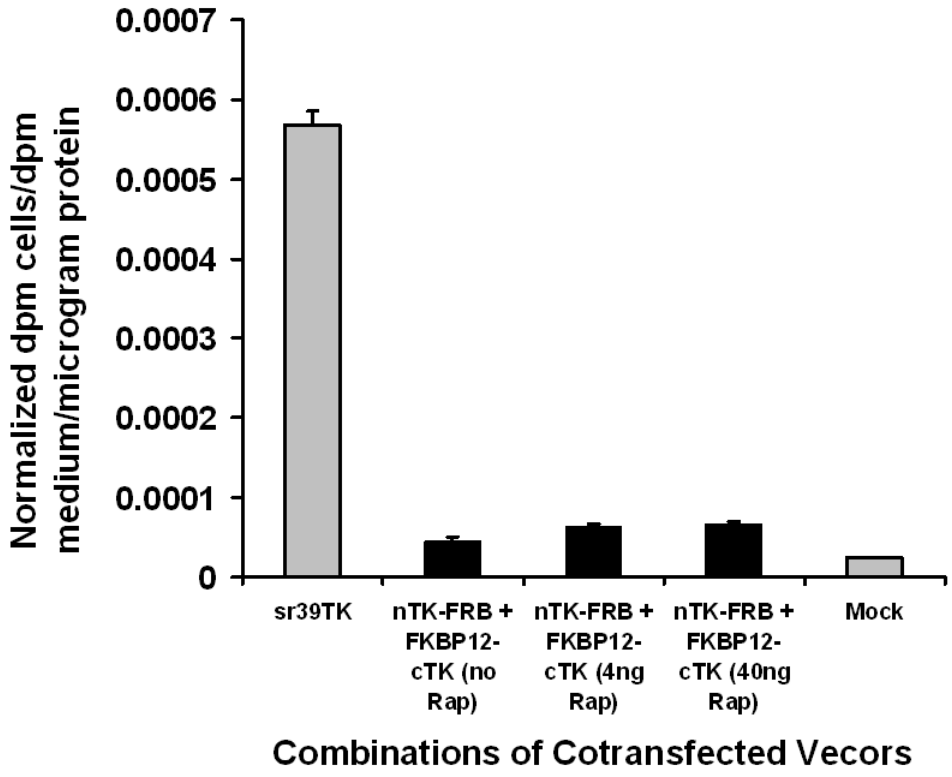

Graph to show comparison of coexpressed chimeras carrying nTK or cTK with FRB/FKBP12 (with and without rapamycin), to study the effect of rapamycin dosage on enzyme activity of a PCA, measured by TK enzyme uptake (expressed as normalized dpm of cells / dpm in medium /microgram of protein) in transiently transfected 293T cells, with mock (negative) and full length HSV1-sr39TK (positive) controls. The error bar is the standard error of the mean for three samples.

Supplementary Fig. 12:

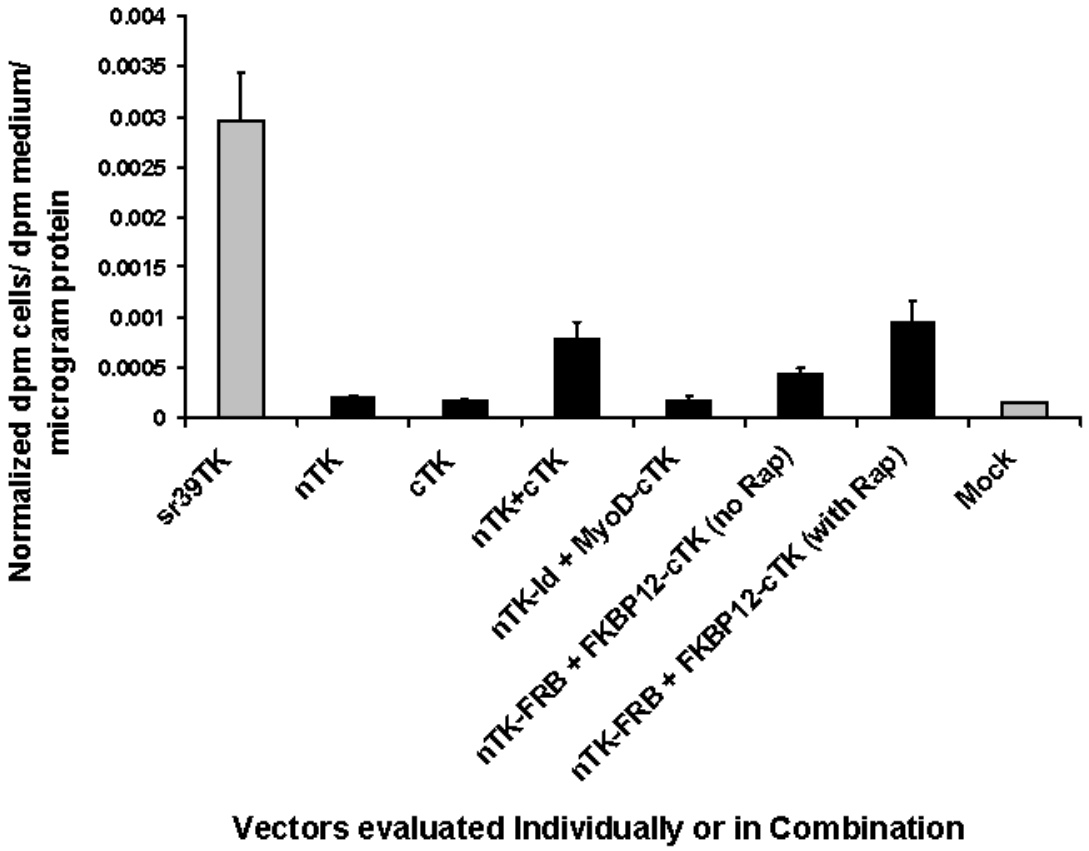

Graph to show comparison of coexpressed chimeras carrying nTK or cTK with FRB/FKBP12 (with and without rapamycin), Id/MyoD, and nTK expressed with cTK (without interacting proteins) on enzyme activity of a PCA, measured by TK enzyme uptake in transiently transfected 293T cells, with mock, nTK alone, and cTK alone as negative controls, and full length HSV1-sr39TK as positive controls. The error bar is the standard error of the mean for three samples.

Supplementary Fig. 13:

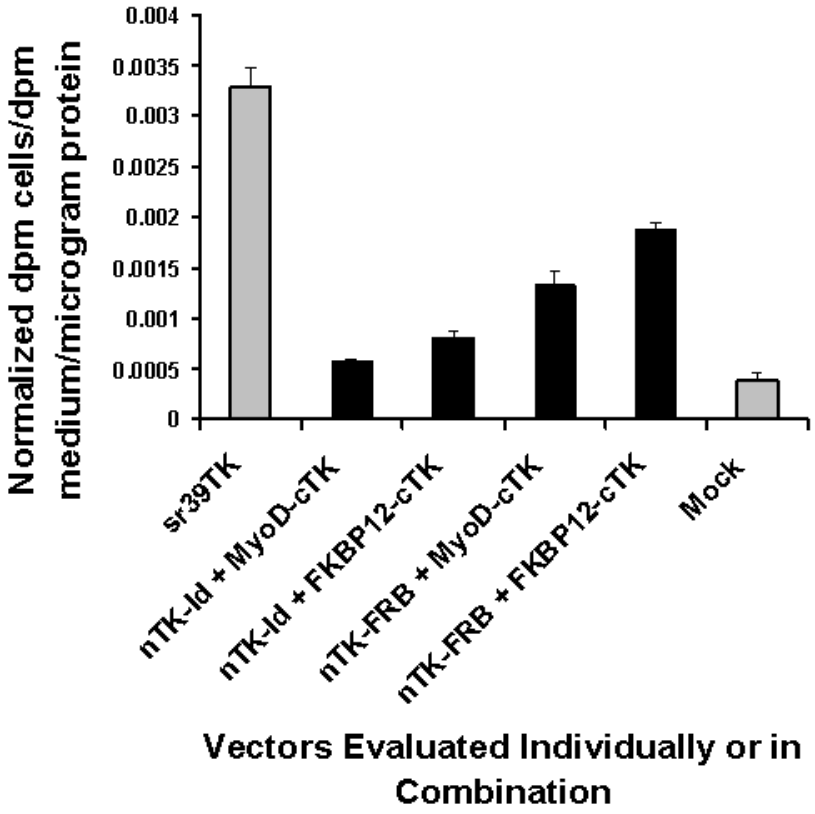

Graph to show comparison of coexpressed chimeras carrying nTK or cTK with FRB/FKBP12 (with and without rapamycin), Id/MyoD, and deliberately mismatched two other sets of chimeras on enzyme activity of a PCA, measured by TK enzyme uptake in transiently transfected 293T cells, with mock (negative) and full length HSV1-sr39TK (positive) controls. The error bar is the standard error of the mean for three samples.

Supplementary Fig. 14:

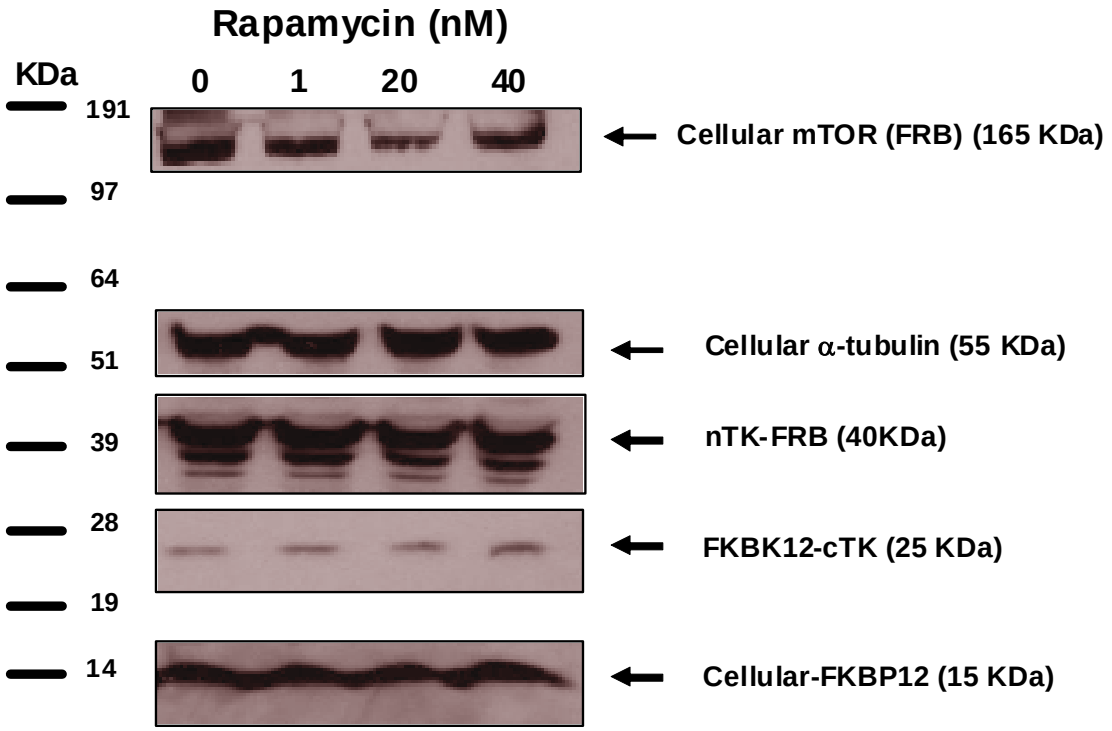

Expression levels of FRB (mTOR) and FKBP12 (in their endogenous and fusion forms) were determined in total lysates of cells transfected with the single vector by immunoblotting with the corresponding antibodies (anti-TK, -FRB, -FKBP12). Anti-α-tubulin was used as an internal control for loading. Cells were exposed to up to 40 nM rapamycin. Anti-mTOR did not reveal a band for expression of nTK-FRB (despite strong α-tubulin expression) likely because of the much smaller size of FRB as compared with the entire mTOR protein. For ease of display and comparison, all three blots were cut and displayed separately relative to the uniform kDa scale provided, although all bands were subjected to similar exposure time and amount of antibody within their own immunoblot. The blot showing cellular mTOR was obtained using antibody to FRB; that showing nTK-FRB and FKBP12-cTK were obtained using antibody to TK; and that showing cellular FKBP12 was obtained using antibody to FKBP12. The uncut blot using antibody to FKBP12 is shown in Supplementary Fig. 15.

Supplementary Fig. 15:

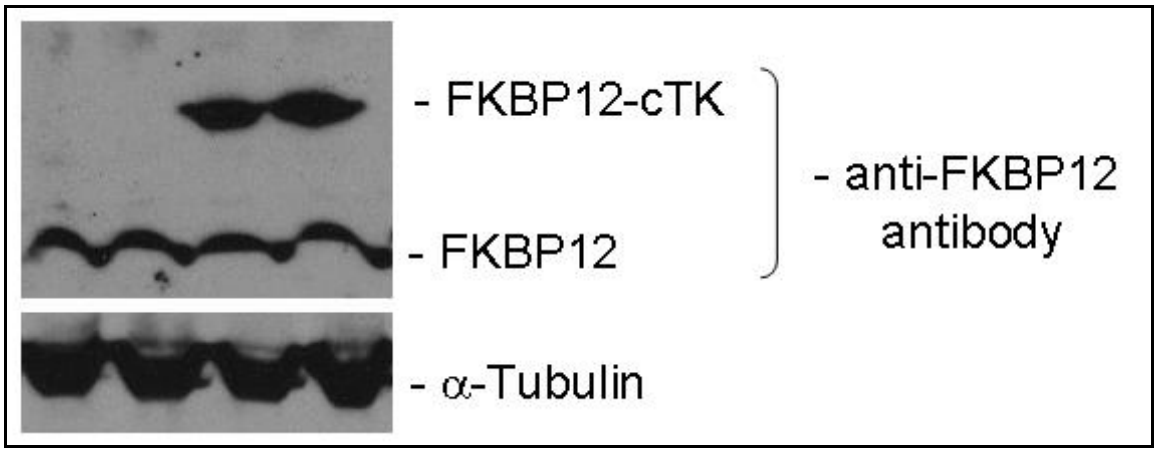

The uncut version of the Western blot showing expression levels of FKBP12 (in their endogenous and fusion forms) as determined in total lysates of cells transfected with the single vector (shown in Supplementary Fig. 4) by immunoblotting with the antibody to FKBP12. Anti-α-tubulin was used as an internal control for loading. Conditions for each of the 4 lanes are exactly as displayed in Supplementary Fig. 14. Optical densitometry of the bands revealed that FKBP12-cTK was expressed at a level only marginally above endogenous cellular FKBP12 (relative band intensities were 1.2:1.0).

Supplementary Fig. 16:

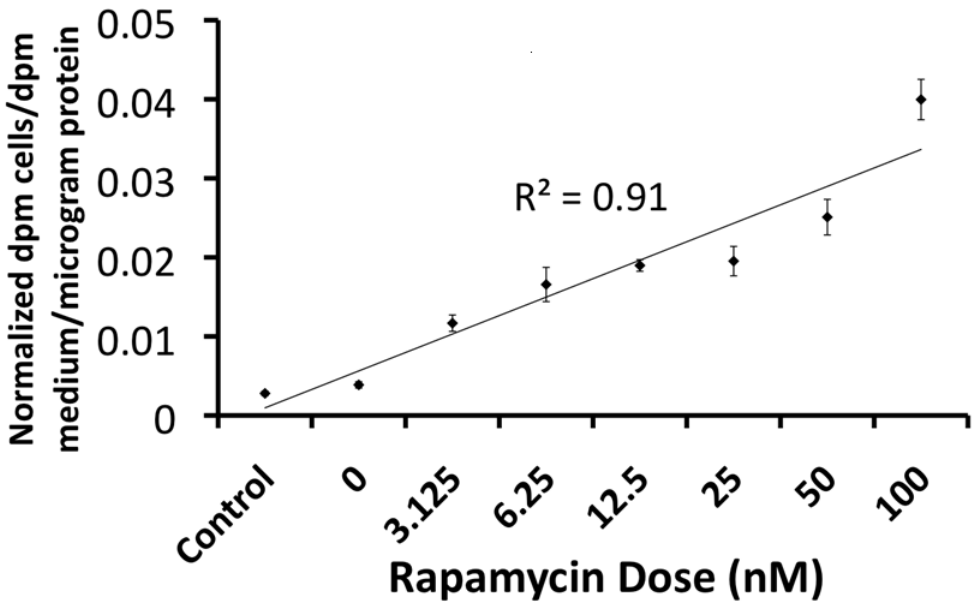

Graph to show in vitro response of 293T cells stably transfected with pcDNA-*p*Ubi-FKBP12-cTK-*p*CMV-nTK$_{(V119C)}$-FRB after 36 h exposure to escalating doses of rapamycin, as measured by TK enzyme uptake (expressed as normalized dpm of cells/dpm in medium/microgram of protein).

Supplementary Fig. 17:

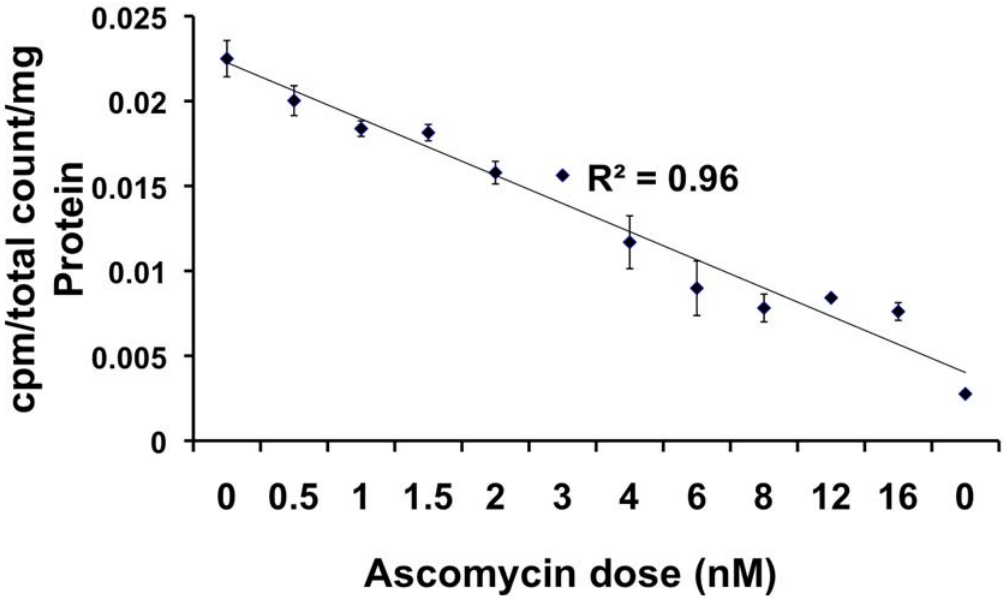

Graph to show in vitro response of 293T cells stably transfected with pcDNA-*p*Ubi-FKBP12-cTK-*p*CMV-nTK$_{(V119C)}$-FRB after 36 h exposure to escalating doses of ascomycin (FK506) along with a fixed 40 nM of rapamycin, as measured by TK enzyme uptake (expressed as normalized dpm of cells/dpm in medium/microgram of protein). An increasing concentration of ascomycin led to a reduction in TK complementation, likely because it blocked the binding of rapamycin to FKBP12 and thus reduced the heterodimerization with FRB.

Supplementary Fig. 18:

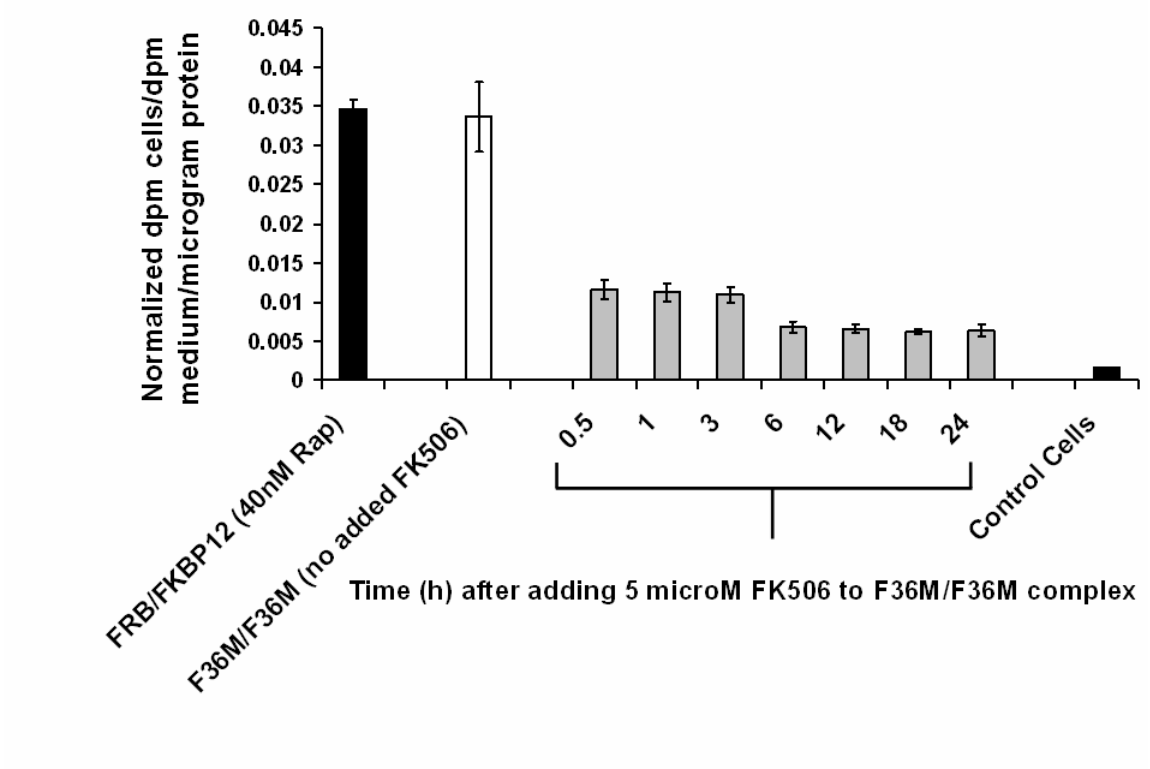

Graph to show reversibility of the split TK-based PCA using a ligand-reversible dimer of a mutant FKBP12 called F_M (F36M) that can be disrupted by FK506. We fused F_M to split TK fragments and transiently expressed the resulting chimeras, $nTK_{(V119C)}$-F_M and F_M-cTK, in a single vector in 293T cells. Twenty-four hours later we added FK506 to these cells and, using an *in vitro* [8-^{3}H]Penciclovir cell uptake assay, measured the time-dependent changes in homodimer complex dissociation and consequent diminished TK complementation. Five μM FK506 resulted in dissociation of about two-thirds of complexes within 30 min. The extent of TK complementation using the F_M homodimer (with no added FK506) was compared initially with that achieved following FRB/FKBP12/rapamycin (Rap) heterodimerization. Control 293T cells carried an empty vector. The error bar is the standard error of the mean for three samples.

Supplementary Fig. 19:

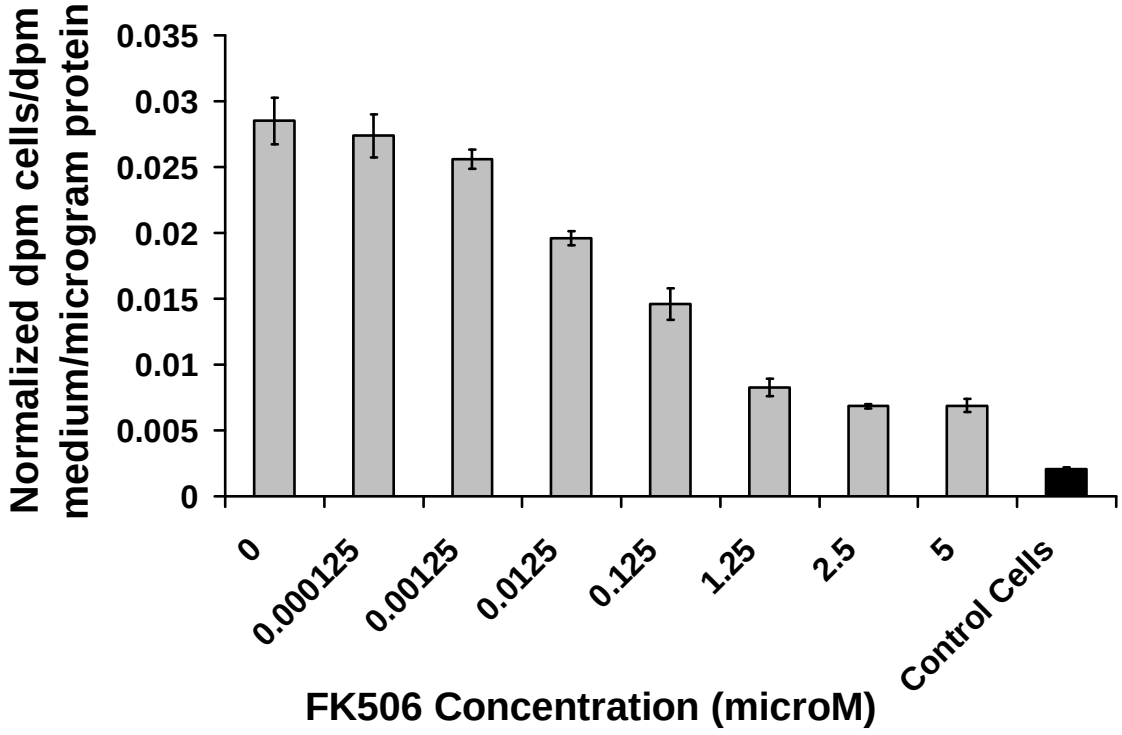

Graph to show reversibility of the split TK-based PCA using a ligand-reversible dimer of a mutant FKBP12 called F_M (F36M) that can be disrupted by FK506. We fused F_M to split TK fragments and transiently expressed the resulting chimeras, $nTK_{(V119C)}$-F_M and F_M-cTK, in a single vector in 293T cells. Twenty-four hours later we added FK506 to these cells and, using an *in vitro* [8-^{3}H]Penciclovir cell uptake assay, measured the dose-dependent changes in homodimer complex dissociation and consequent diminished TK complementation. Incremental reduction of TK activity was observed with increasing doses of FK506 up to 5 μM (measured after 24 hr of exposure to this ligand). Control 293T cells carried an empty vector. The error bar is the standard error of the mean for three samples.

SUPPLEMENTARY TABLES

Table 1

Nucleotide Sequence and the Positions of PCR Primers with Linkers Used for Constructing the Different Expression Vectors in the Study of Circularly Permuted Variants of TK

PRIMER NAME	PRIMER SEQUENCE (5' → 3')	POSITION
Forward nTK	atat **gaattc** gct tcg tac ccc tgc cat caa cac	1-8
Reverse cTK	atat **ggatcc** gtt agc ctc ccc cat ctc ccg ggc	376-369
Reverse nTK_{152}	atat **ctcgag** tca ggc atg tga gct ccc agc ctc ccc	152-145
Forward cTK_{152}	atat **gctagc** atg ccg ccc ccg gcc ctc acc	153-158
Reverse nTK_{180}	atat **ctcgag** tca gcc cat aag gta tcg cgc ggc cgg	180-172
Forward cTK_{180}	atat **gctagc** atg agc atg acc ccc cag gcc gtg ctg	181-188
Reverse nTK_{195}	atat **ctcgag** tca cgg gat gag ggc cac gaa cgc cag	195-188
Forward cTK_{195}	atat **gctagc** atg ccg acc ttg ccc ggc aca aac atc	196-203
Reverse nTK_{265}	atat **ctcgag** tca cgt ccc cga aag ctg tcc cca atc	265-258
Forward cTK_{265}	atat **gctagc** atg gcc gtg ccg ccc cag ggt gcc gag	266-273
Reverse nTK_{300}	atat **ctcgag** tca aac tcg ggg gcc cga aac agg gta	300-293
Forward cTK_{300}	atat **gctagc** atg gct ggc ccc caa cgg cga cct gta	301-308
Forward Linker	**gatcc** ggt ggc gga ggg agc ggt ggc gga ggg agc ggt ggc gga ggg agc g	
Reverse Linker	**aattc** gct ccc tcc gcc acc gct ccc tcc gcc acc gct ccc tcc gcc acc g	

* Bold letters are regions of the restriction enzyme recognition site

Table 2

Nucleotide Sequence of PCR Primers with Linkers Used for Constructing the Different Expression Vectors in the Study of the TK PCA Strategy (with TK split at site 265/266)

PRIMER NAME	PRIMER SEQUENCE (5' → 3')
Forward nTK	atat **gctagc** atg gct tcg tac ccc tgc cat caa
Reverse nTK	atat **gaattc** cgt ccc cga aag ctg tcc cca atc
Forward Id	atat **gaattc** ggt ggc gga ggg agc ggt ggc gga ggg agc cat aaa ttc cca ctt ggt ctg
Reverse Id	atat **ctcgag** att aac cct cac taa agg
Forward MyoD	atat **gctagc** atg ccg gag tgg cag aaa gtt aag acg
Reverse MyoD	atat **ggatcc** gct ccc tcc gcc acc gct ccc tcc gcc acc ccg aat tcg agc tcg ccc ggg
Forward cTK	atat **ggatcc** tgc gtg ccg ccc cag ggt gcc gag ccc
Reverse cTK	atat **ctcgag** tca gtt agc ctc ccc cat ctc ccg

* Bold letters are regions of the restriction enzyme recognition site

SUPPLEMENTARY REFERENCES

1. Massoud, T. F. Novel approaches to molecular imaging of protein-protein interactions in living subjects. PhD thesis, University of Cambridge (2007).
2. Rollins, C.T., et al. A ligand-reversible dimerization system for controlling protein-protein interactions. *Proc. Natl. Acad. Sci. USA* **97**, 7096-7101 (2000).
3. Qi, J., Leahy, R.M., Cherry, S.R., Chatziioannou, A. & Farquhar, T.H. High-resolution 3D Bayesian image reconstruction using the microPET small-animal scanner. *Phys. Med. Biol*. **43**, 1001-1013 (1998).
4. Paulmurugan, R., Umezawa, Y. & Gambhir, S.S. Noninvasive imaging of protein-protein interactions in living subjects by using reporter protein complementation and reconstitution strategies. *Proc. Natl. Acad. Sci. USA* **99**, 15608-15613 (2002).
5. Bhaumik, S. & Gambhir, S.S. Optical imaging of Renilla luciferase reporter gene expression in living mice. *Proc. Natl. Acad. Sci. USA* **99**, 377-382 (2002).
6. Contag, C.H. & Bachmann, M.H. Advances in in vivo bioluminescence imaging of gene expression. *Annu. Rev. Biomed. Eng.* **4**, 235-260 (2002).
7. Ray, P. *et al*. Noninvasive quantitative imaging of protein-protein interactions in living subjects. *Proc. Natl. Acad. Sci. USA* **99**, 3105-3110 (2002).
8. De, A. & Gambhir, S.S. Noninvasive imaging of protein-protein interactions from live cells and living subjects using bioluminescence resonance energy transfer. *FASEB J*. **19**, 2017-2019 (2005).
9. Paulmurugan, R. & Gambhir, S.S. Monitoring protein-protein interactions using split synthetic renilla luciferase protein-fragment-assisted complementation. *Anal. Chem.* **75**, 1584-1589 (2003).
10. Paulmurugan, R., Ray, P., De, A., Chan, C.T. & Gambhir S.S. Imaging protein-protein interactions in living subjects. *Trends. Anal. Chem*. **24**, 446-458 (2005).
11. Massoud, T.F., Paulmurugan, R., De, A., Ray, P. & Gambhir S.S. Reporter gene imaging of protein-protein interactions in living subjects. *Curr. Opin. Biotechnol.* **18**, 31-37 (2007).
12. Luker, G.D., Sharma, V. & Piwnica-Worms, D. Visualizing protein-protein interactions in living animals. *Methods* **29**, 110–122 (2003).
13. Umezawa, Y. Seeing what was unseen: new analytical methods for molecular imaging. *Chem. Rec.* **3**, 22–28 (2003).
14. Ozawa, T. Designing split reporter proteins for analytical tools. *Anal Chim Acta* **556**, 58–68 (2006).
15. Massoud, T.F. & Gambhir, S.S. Molecular imaging in living subjects: seeing fundamental biological processes in a new light. *Genes Devel*. **17**, 545-580 (2003).
16. Jacobs, A. *et al*. Positron-emission tomography of vector-mediated gene expression in gene therapy for gliomas. *Lancet* 358, 727-729 (2001).
17. Penuelas, I. *et al*. Positron emission tomography imaging of adenoviral-mediated transgene expression in liver cancer patients. *Gastroenterology* **128**, 1787-1795 (2005).
18. Dempsey, M.F. *et al*. Assessment of 123I-FIAU imaging of herpes simplex viral gene expression in the treatment of glioma. *Nucl. Med. Commun*. **27**, 611-7 (2006).

19. Gambhir, S.S. Molecular imaging of cancer with positron emission tomography. *Nat. Rev. Cancer* **2**, 683-693 (2002).
20. Penuelas, I. *et al*. Positron emission tomography imaging of adenoviral-mediated transgene expression in liver cancer patients. *Gastroenterology* **128**, 1787-1795 (2005).
21. Luker, G.D. *et al*. Noninvasive imaging of protein-protein interactions in living animals. *Proc. Natl. Acad. Sci. USA* **99**, 6961-6966 (2002).
22. Luker, G.D. *et al*. Molecular imaging of protein-proteion interactions. Controlled expression of p53 and large T-antigen fusion proteins in vivo. *Cancer Res*. **63**, 1780-1788 (2003).
23. Pelletier, J.N., Campbell-Valois, F. & Michnick, S.W. Oligomerization domain-directed reassembly of active dihydrofolate reductase from rationally designed fragments. *Proc. Natl. Acad. Sci. USA* **95**, 12141-12146 (1998).
24. Johnsson, N. & Varshavsky, A. Split ubiquitin as a sensor of protein interactions in vivo. *Proc. Natl. Acad. Sci. USA* **91**, 10340-10344 (1994).
25. Michnick, S.W., Remy, I., Campbell-Valois, F.X., Vallee-Belisle, A. & Pelletier, J.N. Detection of protein-protein interactions by protein fragment complementation strategies. *Methods Enzymol*. **328**, 208-230 (2000).
26. Michnick, S.W. Exploring protein interactions by interaction-induced folding of proteins from complementary peptide fragments. *Curr. Opin. Struct. Biol*. **11**, 472-477 (2001).
27. Ghosh, I., Hamilton, A.D. & Regan, L. Antiparallel leucine zipper-directed protein reassembly: Application to the green fluorescent protein. *J. Am. Chem. Soc.* **122**, 5658-5659 (2000).
28. Graf, R. & Schachman, H.K. Random circular permutation of genes and expressed polypeptide chains: application of the method to the catalytic chains of aspartate transcarbamoylase. *Proc. Natl. Acad. Sci. USA* **93**, 11591-11596 (1996).
29. Christopher, J.A. & Baldwin, T.O. Implications of N and C-terminal proximity for protein folding. *J. Mol. Biol*. 257, 175-187 (1996).
30. Williams, N.K. *et al*. In vivo protein cyclization promoted by a circularly permuted Synechocystis sp. PCC6803 DnaB mini-intein. *J. Biol. Chem*. **277**, 7790-7798 (2002).
31. Wild, K., Bohner, T., Folkers, G. & Schulz, G.E. The structures of thymidine kinase from herpes simplex virus type 1 in complex with substrates and a substrate analogue. *Protein Sci*. **6**, 2097-2106 (1997).
32. Hennecke, J., Sebbel, P. & Glockshuber, R. Random circular permutation of DsbA reveals segments that are essential for protein folding and stability. *J. Mol. Biol.* **286**, 1197-1215 (1999).
33. Iwakura, M., Nakamura, T., Yamane, C. & Maki, K. Systematic circular permutation of an entire protein reveals essential folding elements. *Nat. Struct. Biol.* **7**, 580-585 (2000).
34. Galarneau, A., Primeau, M., Trudeau, L.E. & Michnick, S.W. Beta-lactamase protein fragment complementation assays as in vivo and in vitro sensors of protein protein interactions. *Nat. Biotechnol*. **20**, 619-622 (2002).
35. Gautier, I. *et al*. Homo-FRET microscopy in living cells to measure monomer-dimer transition of GFP-tagged proteins. *Biophys. J*. **80**, 3000-3008 (2001).

36. Paulmurugan, R., Massoud, T.F., Huang, J. & Gambhir, S.S. Molecular imaging of drug-modulated protein-protein interactions in living subjects. *Cancer Res*. **64**, 2113-2119 (2004).
37. Remy, I. & Michnick, S.W. Clonal selection and in vivo quantitation of protein interactions with protein-fragment complementation assays. *Proc. Natl. Acad. Sci. USA* **96**, 5394-5399 (1999).
38. Kaufman, R.J., Bertino, J.R. & Schinke, R.T. Quantitation of dihydrofolate reductase in individual parental and methotrexate-resistant murine cells. Use of a fluorescence activated cell sorter. *J. Biol. Chem*. **253**, 5852-5860 (1978).
39. Argent™ Regulated heterodimerization Kit, Version 2.0, ARIAD Pharmaceuticals, 5. Inc. (2002).
40. Langlands, K., Yin, X., Anand, G. & Prochownik, E.V. Differential interactions of Id proteins with basic-helix-loop-helix transcription factors. *J. Biol. Chem.* **272**, 19785-19793 (1997).
41. Paulmurugan, R. & Gambhir S.S. Firefly luciferase enzyme fragment complementation for imaging in cells and living animals. *Anal. Chem*. **77**, 1295-1302 (2005).
42. Hu, C.D. & Kerppola, T.K. Simultaneous visualization of multiple protein interactions in living cells using multicolor fluorescence complementation analysis. *Nat. Biotechnol*. **21**, 539-545 (2003).
43. Degreve, B., Esnouf, R., De Clercq, E. & Balzarini, J. Characterization of multiple nuclear localization signals in herpes simplex virus type 1 thymidine kinase. *Biochem. Biophys. Res. Comm*. **264**, 338-342 (1999).
44. Wurth, C., Thomas, R.M., Folkers, G. & Scapozza, L. Folding and self-assembly of herpes simplex virus type 1 thymidine kinase. *J. Mol. Biol*. **313**, 657-670 (2001).
45. Chen, J. & Schreiber, S.L. Identification of an 11-kDa FKBP12-rapamycin-binding domain within the 289-kDa FKBP12-rapamycin-associated protein and characterization of a critical serine residue. *Proc. Natl. Acad. Sci. USA* **92**, 4947-4951 (1995).
46. Banaszynski, L.A., Liu, C.W. & Wandless, T.J. Characterization of the FKBP.rapamycin.FRB ternary complex. *J. Am. Chem. Soc*. **127**, 4715-4721 (2005).
47. Remy, I. & Michnick, S.W. A highly sensitive protein-protein interaction assay based on *Gaussia* luciferase. *Nat. Methods* **3**, 977-979 (2006).
48. Paulmurugan, R. & Gambhir S.S. Novel fusion protein approach for efficient high-throughput screening of small molecule-mediating protein-protein interactions in cells and living animals. *Cancer Res*. **65**, 7413-20 (2005).